SAPIENZA
UNIVERSITÀ DI ROMA

Robotics and Automation Seminars
Pisa, January 12, 2023

New Results on Fault and Collision Detection in Robot Manipulators

Alessandro De Luca
DIAG, Sapienza Università di Roma

Previous work: mainly with **Raffaella Mattone, Sami Haddadin, Fabrizio Flacco†, Claudio Gaz**

New results: include also joint work with **Andrea Cristofaro, Claudio Gaz, Lorenzo Govoni, Pasquale Palumbo, Marco Pennese**

Summary

Detection and isolation of fault events for different classes of robots

- actuator failures and link collisions in robots can both be handled as **system faults**
  - fault detection
  - … and isolation (FDI)
  - identification of time profiles and classification of fault severity
- **review** of FDI results for robot manipulators with **rigid links** or with **elastic joints**
  - model-based residual methods
  - monitoring energy (only for detection) or generalized momentum (also for isolation)
  - without or with joint torque sensing
- **new** results
  - position-based residual for collisions in **rigid robots**
    - using a novel reduced-order observer for velocity (with experiments on KUKA LWR4 robot)
  - momentum-based residual for collisions in the general class of **robots with elastic joints**
    - with motor-link inertia couplings (Tomei model vs. Spong model)
  - residuals for actuator fault & collision in a **robot with a flexible link (Flexarm)**
    - detection and isolation results with full state measurements
    - detection using a nonlinear observer to estimate modal deformation variables and their rates

Rigid robots

Actuator faults – FDI

dynamic model

$$\boldsymbol{M}(\boldsymbol{q})\ddot{\boldsymbol{q}} + \boldsymbol{c}(\boldsymbol{q},\dot{\boldsymbol{q}}) + \boldsymbol{g}(\boldsymbol{q}) + \boldsymbol{f}(\boldsymbol{q},\dot{\boldsymbol{q}}) = \boldsymbol{\tau} + \boldsymbol{\tau}_F$$

friction — actuator faults (of any nature)

generalized momentum (and its dynamics)

$$\begin{cases} \boldsymbol{p} = \boldsymbol{M}(\boldsymbol{q})\dot{\boldsymbol{q}} \\ \dot{\boldsymbol{p}} = \boldsymbol{\tau} + \boldsymbol{\tau}_F - \boldsymbol{\alpha}(\boldsymbol{q},\dot{\boldsymbol{q}}) \\ \alpha_i = -\dfrac{1}{2}\dot{\boldsymbol{q}}^T \dfrac{\partial \boldsymbol{M}}{\partial q_i}\dot{\boldsymbol{q}} + g_i(\boldsymbol{q}) + f_i(q_i,\dot{q}_i) \qquad i = 1,\ldots,n \end{cases}$$

residual vector

$$\boldsymbol{r}(t) = \boldsymbol{K}_r\left(\boldsymbol{p} - \int_0^t (\boldsymbol{\tau} - \boldsymbol{\alpha}(\boldsymbol{q},\dot{\boldsymbol{q}}) + \boldsymbol{r})\, ds\right) \qquad \boldsymbol{K}_r > 0, \text{diagonal}$$

FDI property of the residual

$$\begin{cases} \dot{\boldsymbol{r}} = \boldsymbol{K}_r(\boldsymbol{\tau}_F - \boldsymbol{r}) \\ \dot{r}_i = K_{r,i}(\tau_{F,i} - r_i) \qquad i = 1,\ldots,n \end{cases}$$

⇒ **one-to-one** (decoupled!) mapping

A. De Luca, R. Mattone "Actuator failure detection and isolation using generalized momenta" ICRA 2003

Residual generator

Block diagram as a disturbance observer (first-order filtered estimate of $\boldsymbol{\tau}_F$)

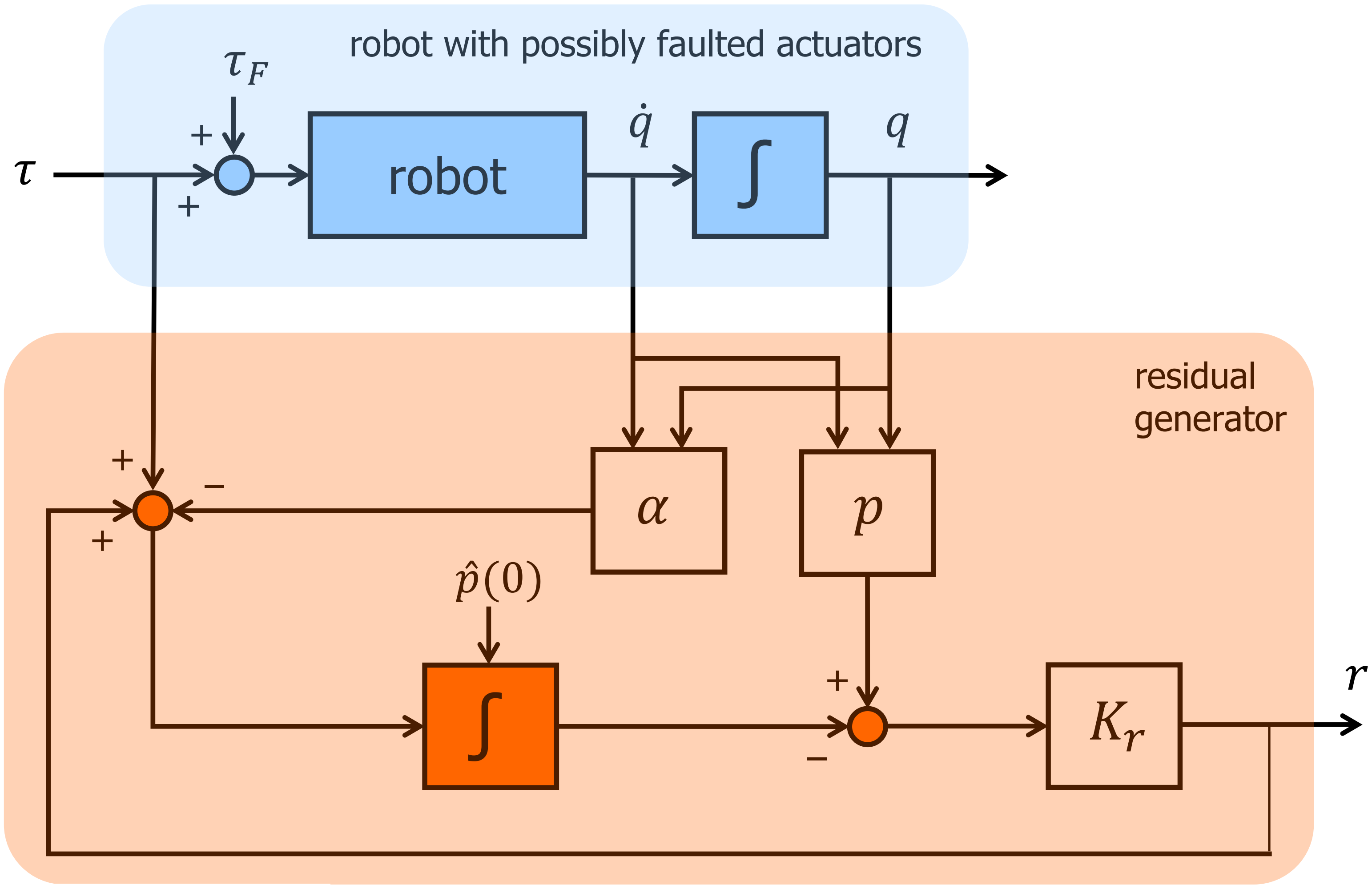

initialization of integrators $\hat{p}(0) = p(0)$ (zero if robot starts at rest)

$$\dot{\hat{\boldsymbol{p}}} = \boldsymbol{\tau} - \boldsymbol{\alpha}(\boldsymbol{q}, \dot{\boldsymbol{q}}) + \boldsymbol{K}_r\,(\boldsymbol{p} - \hat{\boldsymbol{p}})$$

$$\boldsymbol{r} = \boldsymbol{K}_r\,(\boldsymbol{p} - \hat{\boldsymbol{p}})$$

$$\boldsymbol{e}_{obs} = \boldsymbol{\tau}_F - \boldsymbol{r} \quad \Rightarrow \quad \dot{\boldsymbol{e}}_{obs} = \dot{\boldsymbol{\tau}}_F - \boldsymbol{K}_r\boldsymbol{e}_{obs} \simeq -\boldsymbol{K}_r\boldsymbol{e}_{obs}$$

Actuator FDI

Experimental results on a Pendubot (2R robot, underactuated)

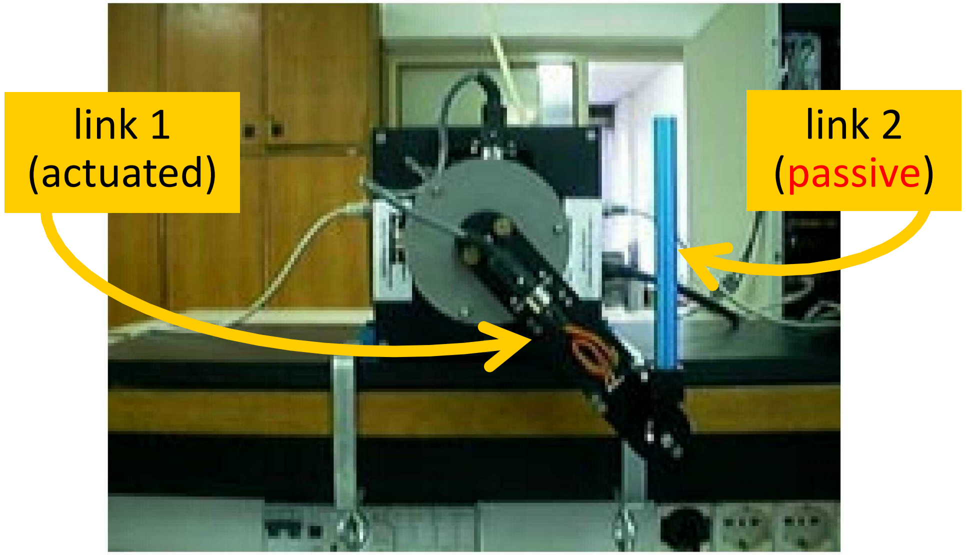

one motor (joint 1), encoders at both joints

- motor 1 is driven by a sinusoidal voltage of period 2π sec (in open loop)
- bias fault on τ_1 for $t \in [3 \div 4]$ s
- total fault on joint 2 for $t \in [3.5 \div 4.5]$ s
- fault concurrency for $t \in [3.5 \div 4]$ s

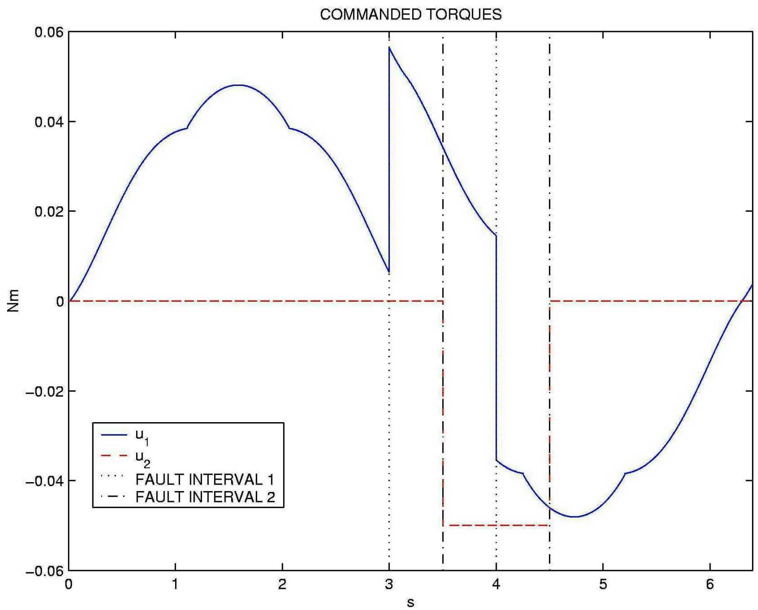

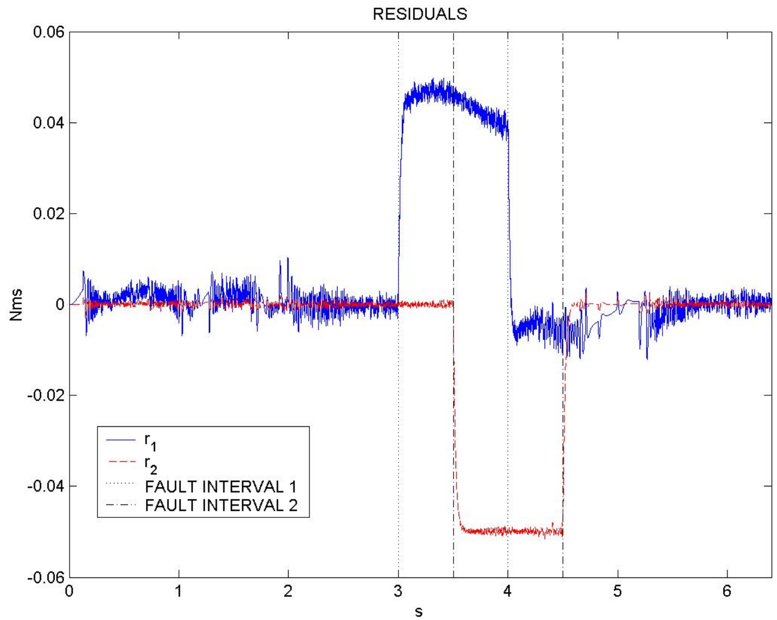

Robot collision events

From coexistence to safe reaction and collaboration

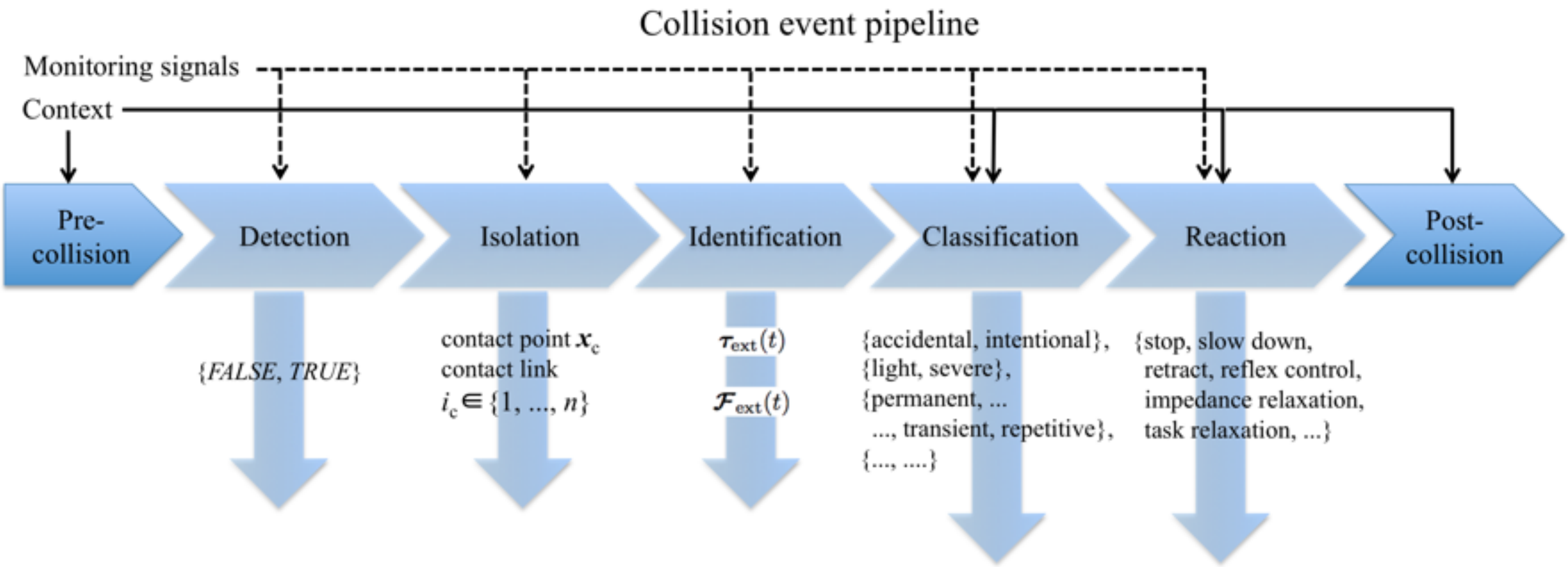

S. Haddadin, A. De Luca, A. Albu-Schäffer "Robot collisions: A survey on detection, isolation, and identification" IEEE Transactions on Robotics 2017

Rigid robots

Link collisions – FDI

dynamic model (with factorization)

$$\boldsymbol{M}(\boldsymbol{q})\ddot{\boldsymbol{q}} + \boldsymbol{S}(\boldsymbol{q},\dot{\boldsymbol{q}})\dot{\boldsymbol{q}} + \boldsymbol{g}(\boldsymbol{q}) + \boldsymbol{f}(\boldsymbol{q},\dot{\boldsymbol{q}}) = \boldsymbol{\tau} + \boldsymbol{\tau}_C$$

Coriolis/centrifugal — friction — joint torques due to link collision (anywhere, any time)

skew-symmetric property in momentum dynamics

$$\begin{cases} \dot{\boldsymbol{M}}(\boldsymbol{q}) = \boldsymbol{S}(\boldsymbol{q},\dot{\boldsymbol{q}}) + \boldsymbol{S}^T(\boldsymbol{q},\dot{\boldsymbol{q}}) \\ \dot{\boldsymbol{p}} = \boldsymbol{\tau} + \boldsymbol{\tau}_C + \boldsymbol{S}^T(\boldsymbol{q},\dot{\boldsymbol{q}})\dot{\boldsymbol{q}} - \boldsymbol{g}(\boldsymbol{q}) - \boldsymbol{f}(\boldsymbol{q},\dot{\boldsymbol{q}}) \end{cases}$$

$$\boldsymbol{\tau}_C \,(= \boldsymbol{\tau}_F) = \boldsymbol{J}_C^T(\boldsymbol{q})\boldsymbol{F}_C$$

residual vector

$$\boldsymbol{r}(t) = \boldsymbol{K}_r \left(\boldsymbol{p} - \int_0^t \left(\boldsymbol{\tau} + \boldsymbol{S}^T(\boldsymbol{q},\dot{\boldsymbol{q}})\dot{\boldsymbol{q}} - \boldsymbol{g}(\boldsymbol{q}) - \boldsymbol{f}(\boldsymbol{q},\dot{\boldsymbol{q}}) + \boldsymbol{r} \right) ds \right)$$

$$\boldsymbol{K}_r > 0, \text{diagonal}$$

FDI property of the residual

$$\dot{\boldsymbol{r}} = \boldsymbol{K}_r \left(\boldsymbol{\tau}_C - \boldsymbol{r} \right)$$

⇒ colliding link = largest **index** of residual component exceeding a detection threshold

A. De Luca, R. Mattone "Sensorless robot collision detection and hybrid force/motion control" ICRA 2005

A. De Luca, A. Albu-Schäffer, S. Haddadin, G. Hirzinger "Collision detection and safe reaction with the DLR-III lightweight manipulator arm" IROS 2006

Isolation of link collisions

Experiment with a position-controlled DLR LWR-III 7R robot while three links are in motion

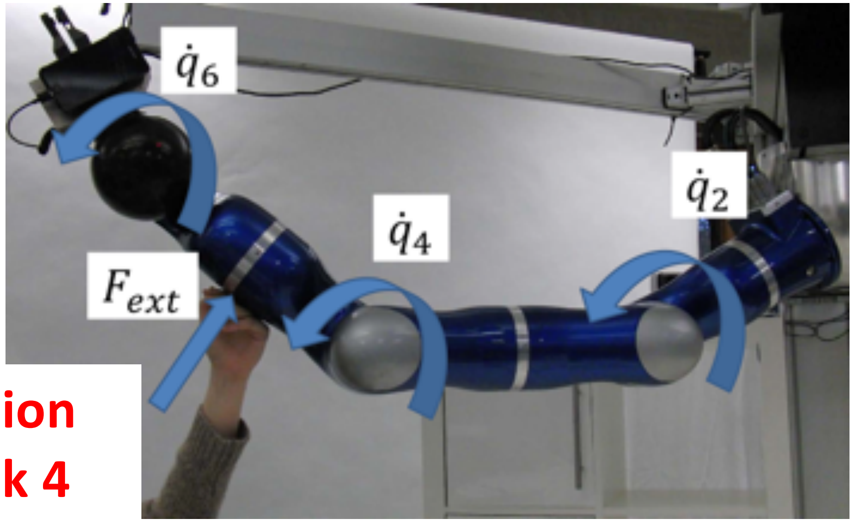

collision at link 4

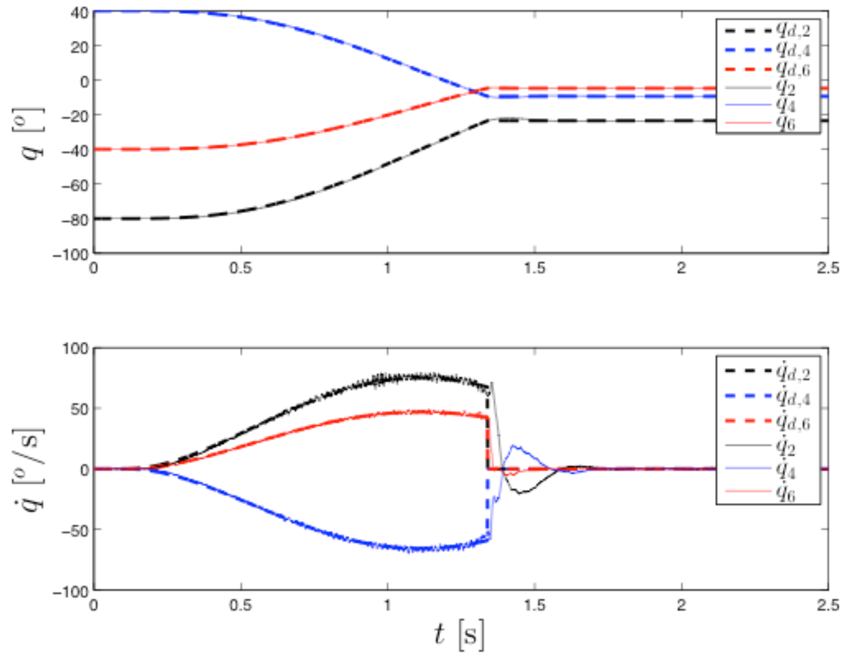

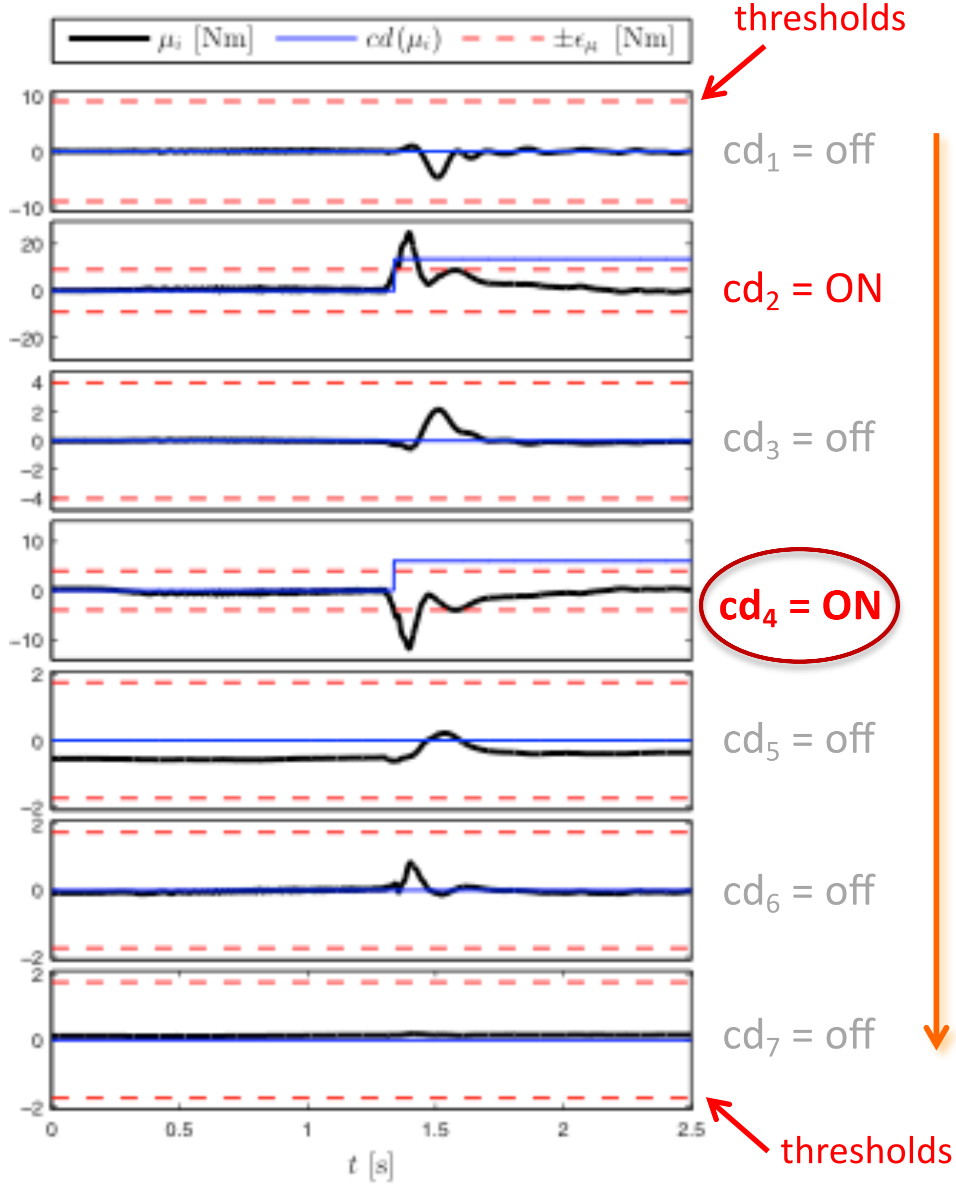

Rigid robots

Link collisions – Detection only (but a simpler scalar residual)

total robot energy

$$E = T + U_g = \frac{1}{2}\dot{\boldsymbol{q}}^T \boldsymbol{M}(\boldsymbol{q})\dot{\boldsymbol{q}} + U_g(\boldsymbol{q})$$

kinetic gravitational

... and its dynamics

$$\dot{E} = \dot{\boldsymbol{q}}^T \left(\boldsymbol{\tau} + \boldsymbol{\tau}_C - \boldsymbol{f}(\boldsymbol{q}, \dot{\boldsymbol{q}})\right)$$

scalar residual

$$\sigma = k_\sigma \left(E - \int_0^t \left(\dot{\boldsymbol{q}}^T \left(\boldsymbol{\tau} - \boldsymbol{f}(\boldsymbol{q}, \dot{\boldsymbol{q}})\right) + \sigma\right) ds \right) \qquad k_\sigma > 0$$

detection only (and with robot in motion!)

$$\dot{\sigma} = k_\sigma \left(\dot{\boldsymbol{q}}^T \boldsymbol{\tau}_C - \sigma\right)$$

- scalar and vector residuals σ and $\boldsymbol{r}$ can be **used together** to improve thresholding performance in avoiding false positive or false negative collision events …

A. De Luca, A. Albu-Schäffer, S. Haddadin, G. Hirzinger “Collision detection and safe reaction with the DLR-III lightweight manipulator arm” IROS 2006

Link collisions

Experiments on a Neura LARA 5 cobot (rigid model, no joint torque sensors)

video

D. Zurlo, T. Heitmann, M. Morlock, A. De Luca "Collision detection and contact point estimation using virtual joint torque sensing applied to a cobot" submitted to ICRA 2023

Sources of joint elasticity

Harmonic Drives in the DLR-KUKA LWR series of lightweight collaborative robots

$$\boldsymbol{\tau}_J = \boldsymbol{K}(\boldsymbol{\theta} - \boldsymbol{q})$$

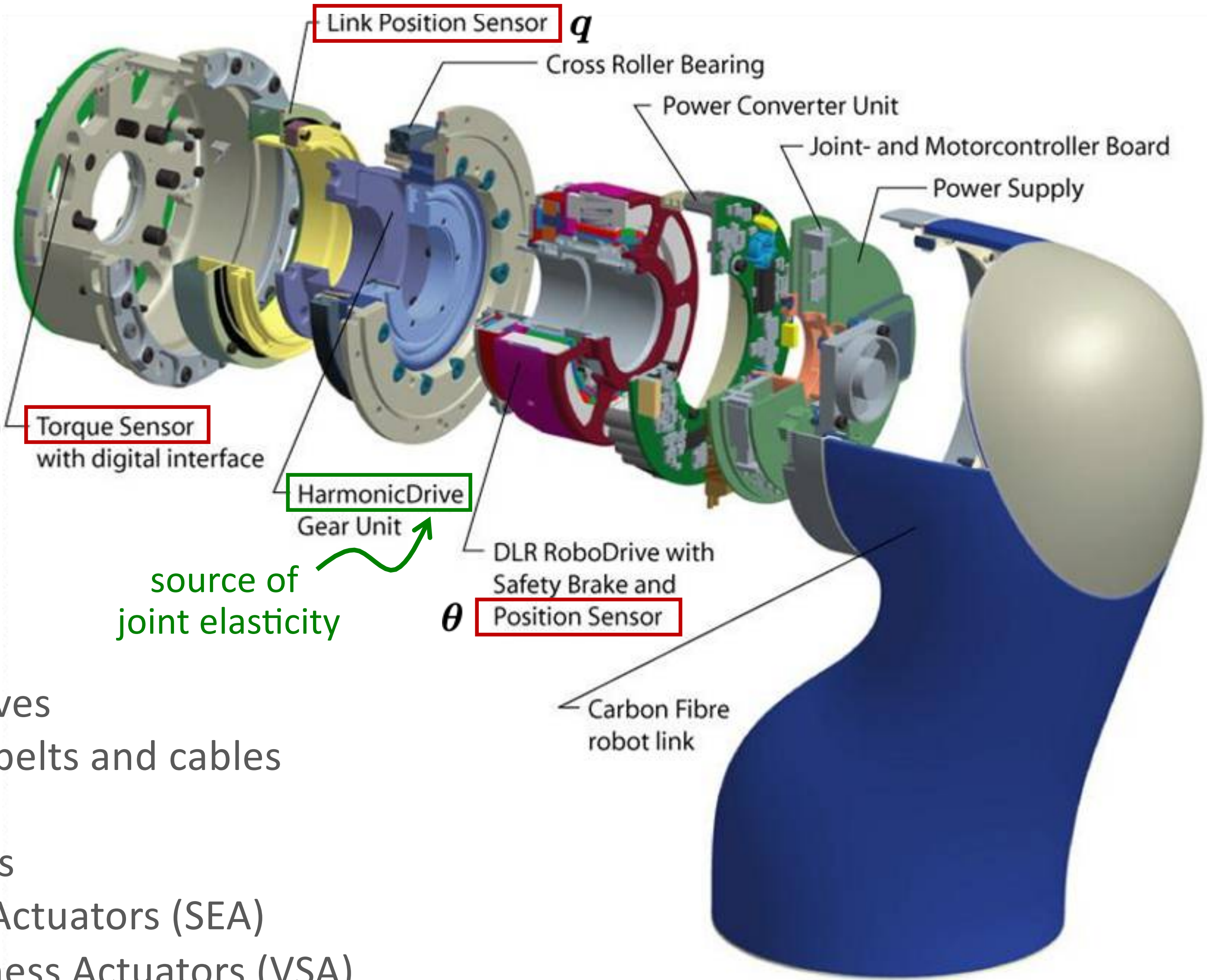

- Harmonic Drives
- transmission belts and cables
- long shafts
- cycloidal gears
- Serial Elastic Actuators (SEA)
- Variable Stiffness Actuators (VSA)

Robots with elastic joints

Dynamic model and properties

dynamic model (with **Spong** simplifying assumption)

$$\begin{cases} \boldsymbol{M}(\boldsymbol{q})\ddot{\boldsymbol{q}} + \boldsymbol{S}(\boldsymbol{q},\dot{\boldsymbol{q}})\dot{\boldsymbol{q}} + \boldsymbol{g}(\boldsymbol{q}) = \boldsymbol{\tau}_J + \boldsymbol{\tau}_C \\ \boldsymbol{M}_m\ddot{\boldsymbol{\theta}} + \boldsymbol{f}_m(\boldsymbol{q},\dot{\boldsymbol{q}}) + \boldsymbol{\tau}_J = \boldsymbol{\tau} \end{cases}$$

link equation

motor equation

motor friction

$$\boldsymbol{\tau}_J = \boldsymbol{K}(\boldsymbol{\theta} - \boldsymbol{q})$$

joint elastic torque

generalized momentum

$$\boldsymbol{p} = \begin{pmatrix} \boldsymbol{p}_q \\ \boldsymbol{p}_\theta \end{pmatrix} = \begin{pmatrix} \boldsymbol{M}(\boldsymbol{q})\dot{\boldsymbol{q}} \\ \boldsymbol{M}_m\dot{\boldsymbol{\theta}} \end{pmatrix}$$

$$\boldsymbol{p}_q = \boldsymbol{M}(\boldsymbol{q})\dot{\boldsymbol{q}} \; (= \boldsymbol{p} \text{ of the rigid case})$$

$$\dot{\boldsymbol{p}}_\theta = \boldsymbol{\tau} - \boldsymbol{\tau}_J - \boldsymbol{f}_m(\boldsymbol{q},\dot{\boldsymbol{q}})$$

total robot energy

$$E_{EJ} = T_q + T_m + U_g + U_e$$
$$= \frac{1}{2}\dot{\boldsymbol{q}}^T\boldsymbol{M}(\boldsymbol{q})\dot{\boldsymbol{q}} + \frac{1}{2}\dot{\boldsymbol{\theta}}^T\boldsymbol{M}_m\dot{\boldsymbol{\theta}} + U_g(\boldsymbol{q}) + \frac{1}{2}(\boldsymbol{\theta}-\boldsymbol{q})^T\boldsymbol{K}(\boldsymbol{\theta}-\boldsymbol{q})$$

elastic energy

$$E_q = T_q + U_g \; (= E \text{ of the rigid case})$$

$$\dot{E}_{EJ} = \dot{\boldsymbol{q}}^T\boldsymbol{\tau}_C + \dot{\boldsymbol{\theta}}^T(\boldsymbol{\tau} - \boldsymbol{f}(\boldsymbol{q},\dot{\boldsymbol{q}}))$$

A. De Luca, W. Book "Robot with flexible elements" Chapter 11 in B. Siciliano, O. Khatib (Eds.) Springer Handbook of Robotics 2016

Robots with elastic joints

Link collisions – alternatives for vector and scalar residuals

$$\boldsymbol{r}_{EJ}(t) = \boldsymbol{K}_r \left(\boldsymbol{p}_q - \int_0^t \left(\boldsymbol{\tau}_J + \boldsymbol{S}^T(\boldsymbol{q},\dot{\boldsymbol{q}})\dot{\boldsymbol{q}} - \boldsymbol{g}(\boldsymbol{q}) + \boldsymbol{r}_{EJ} \right) ds \right)$$

$$\boldsymbol{r}_{EJ}(t) = \boldsymbol{K}_r \left(\boldsymbol{p}_q - \int_0^t \left(\boldsymbol{K}(\boldsymbol{\theta} - \boldsymbol{q}) + \boldsymbol{S}^T(\boldsymbol{q},\dot{\boldsymbol{q}})\dot{\boldsymbol{q}} - \boldsymbol{g}(\boldsymbol{q}) + \boldsymbol{r}_{EJ} \right) ds \right)$$

$$\boldsymbol{r}_{EJ}(t) = \boldsymbol{K}_r \left(\boldsymbol{p}_q + \boldsymbol{p}_\theta - \int_0^t \left(\boldsymbol{\tau} + \boldsymbol{S}^T(\boldsymbol{q},\dot{\boldsymbol{q}})\dot{\boldsymbol{q}} - \boldsymbol{g}(\boldsymbol{q}) - \boldsymbol{f}_m(\boldsymbol{q},\dot{\boldsymbol{q}}) + \boldsymbol{r}_{EJ} \right) ds \right)$$

FDI property

$$\dot{\boldsymbol{r}}_{EJ} = \boldsymbol{K}_r \left(\boldsymbol{\tau}_C - \boldsymbol{r}_{EJ} \right)$$

no use of joint stiffness (good also for **VSA**!)

$$\sigma_{EJ}(t) = k_\sigma \left(E_q - \int_0^t \left(\dot{\boldsymbol{q}}^T \boldsymbol{\tau}_J + \sigma_{EJ} \right) ds \right)$$

$$\sigma_{EJ}(t) = k_\sigma \left(E_q - \int_0^t \left(\dot{\boldsymbol{q}}^T \boldsymbol{K}(\boldsymbol{\theta} - \boldsymbol{q}) + \sigma_{EJ} \right) ds \right)$$

$$\sigma_{EJ}(t) = k_\sigma \left(E_{EJ} - \int_0^t \left(\dot{\boldsymbol{\theta}}^T \left(\boldsymbol{\tau} - \boldsymbol{f}_m(\boldsymbol{q},\dot{\boldsymbol{q}}) \right) + \sigma_{EJ} \right) ds \right)$$

no need of joint torque sensors (best for **SEA**!)

$$\dot{\sigma}_{EJ} = k_\sigma \left(\dot{\boldsymbol{q}}^T \boldsymbol{\tau}_C - \sigma_{EJ} \right)$$

detection only (with robot in motion)

S. Haddadin, A. Albu-Schäffer, A. De Luca, G. Hirzinger "Collision detection and reaction: A contribution to safe physical human-robot interaction" IROS 2008 (Best Application Paper Award)

S. Haddadin, A. De Luca, A. Albu-Schäffer "Robot collisions: A survey on detection, isolation, and identification" IEEE Transactions on Robotics 2017

Collision detection and reaction

Portfolio of possible robot behaviors implemented on different systems (5 videos)

the early days (2005-08) …

IROS 2016 (KUKA LWR4)

Mechatronics 2018 (UR 10)

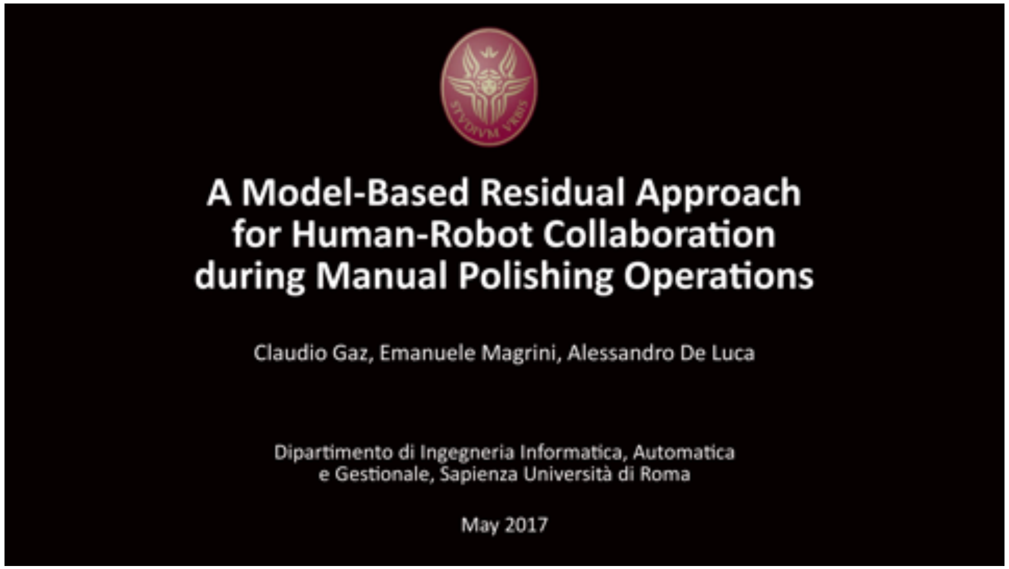

I-RIM 2021 (KUKA KR5)

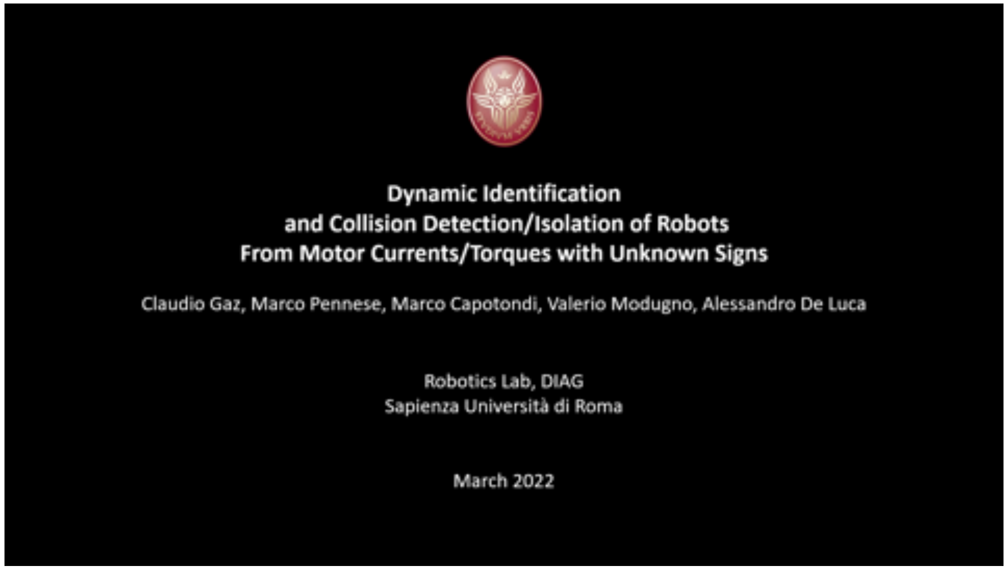

Reduced-order velocity observer for rigid robots

Avoiding numerical differentiation of encoder positions

- to be used in output feedback control laws and for collision detection/isolation
- nice to have the same first-order structure of momentum-based residual
- should work in closed-loop or open-loop mode (with possibly unbounded velocity)

$$\boldsymbol{M}(\boldsymbol{q})\dot{\boldsymbol{z}} = \boldsymbol{\tau} - \boldsymbol{S}(\boldsymbol{q},\hat{\dot{\boldsymbol{q}}})\,\hat{\dot{\boldsymbol{q}}} - \boldsymbol{g}(\boldsymbol{q}) - \boldsymbol{f}(\boldsymbol{q},\hat{\dot{\boldsymbol{q}}}) - k_0\,\boldsymbol{M}(\boldsymbol{q})\hat{\dot{\boldsymbol{q}}}$$

$$\hat{\dot{\boldsymbol{q}}} = \boldsymbol{z} + k_0\,\boldsymbol{q}$$

Theorem 1. Assume that $\|\dot{q}\| \leq v_{max}$ is known. Then, for any fixed $\eta > 0$, by choosing

$$k_0 \geq (c_0 v_{max} + \eta)/\lambda_{min}(\boldsymbol{M}(\boldsymbol{q}))$$

we obtain **local exponential stability** of the observation error $\boldsymbol{\varepsilon} = \dot{\boldsymbol{q}} - \hat{\dot{\boldsymbol{q}}}$ with a region of attraction $\mathcal{E}(\eta)$.

Theorem 2. Assume that $\limsup_{n\to\infty} \|\dot{q}\| \leq v$ exists but is yet unknown. Then, using a switching logic to adjust the gain with a hybrid dynamics scheme, we obtain **local exponential stability** of the observation error $\boldsymbol{\varepsilon} = \dot{\boldsymbol{q}} - \hat{\dot{\boldsymbol{q}}}$.

A. Cristofaro, A. De Luca "Reduced-order observer design for robot manipulators" IEEE Control Systems Letters 2023 (online Nov 2022)

Velocity observer for rigid robots

Comparative simulations on a 2R planar robot under gravity

- **faster** convergence than with full-order observer (e.g., Nicosia-Tomei IEEE T-AC 1990)
- **robust** with respect to noisy measurements and model uncertainties

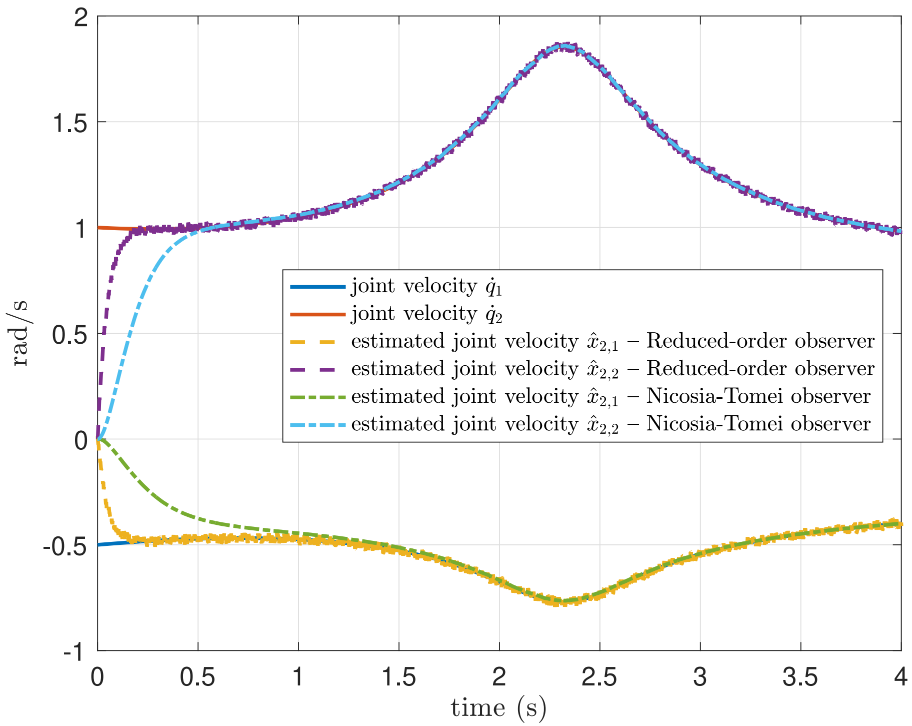

presence of noise and quantization

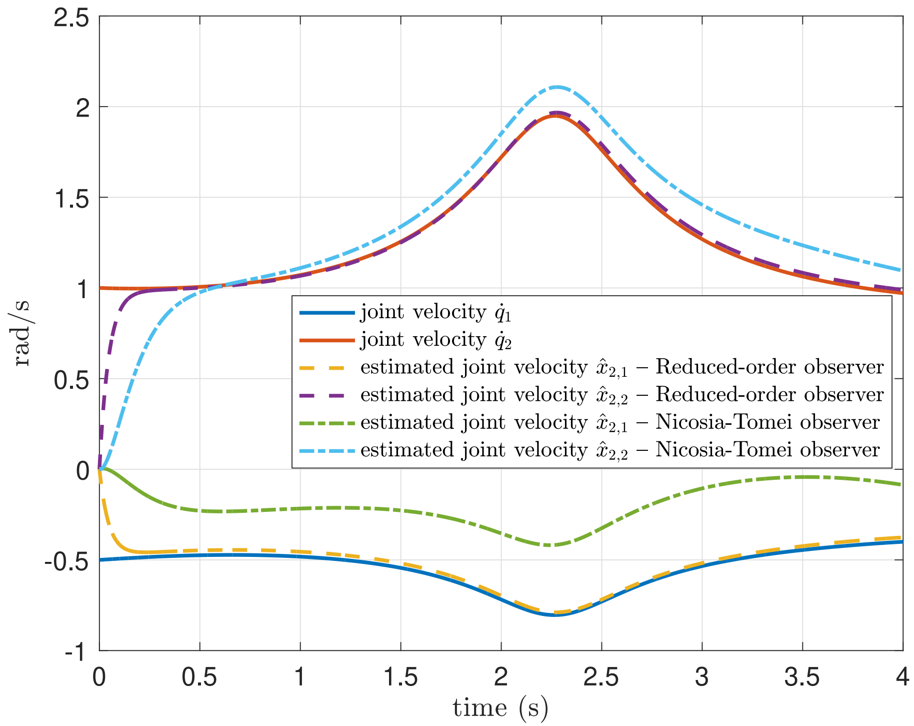

10% error on both link masses

$$\boldsymbol{\tau} = \boldsymbol{g}(\boldsymbol{q}) + \begin{pmatrix} \cos(t/2) \\ -\cos t \end{pmatrix}$$

Use of position-based residual for collisions

Experiments on a KUKA LWR4 with momentum-based residual using the velocity observer

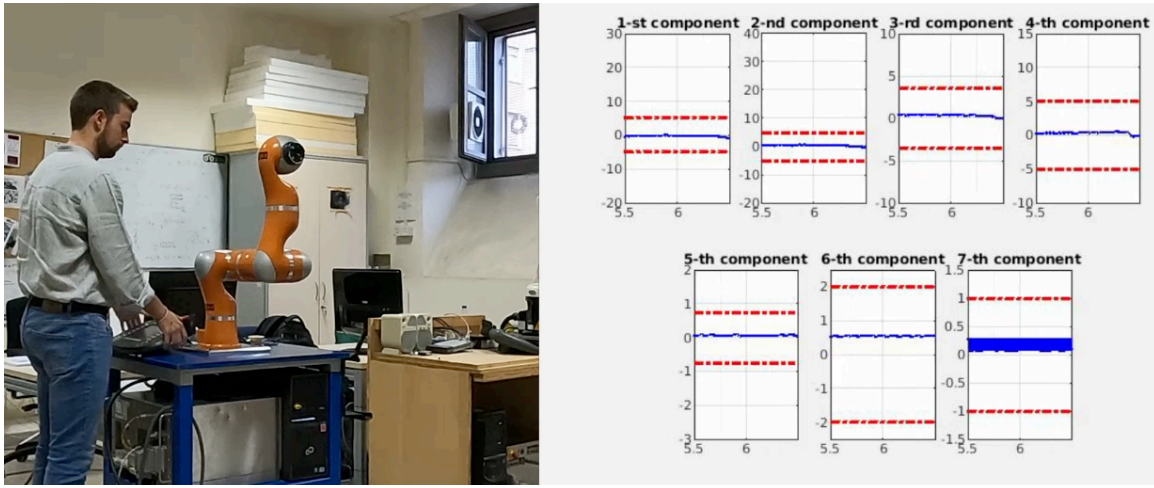

- numerical differentiation vs. observer
- 6 link collisions in sequence (over 30 s):

L4 (twice, ±) ⇒ L5 (twice, ±) ⇒ L2 (twice, ±)

- both methods detect collisions correctly
- ND has two false isolations (#5 and #6)
- OBS isolates the colliding link correctly

video

only first 5 residuals are shown (out of 7)

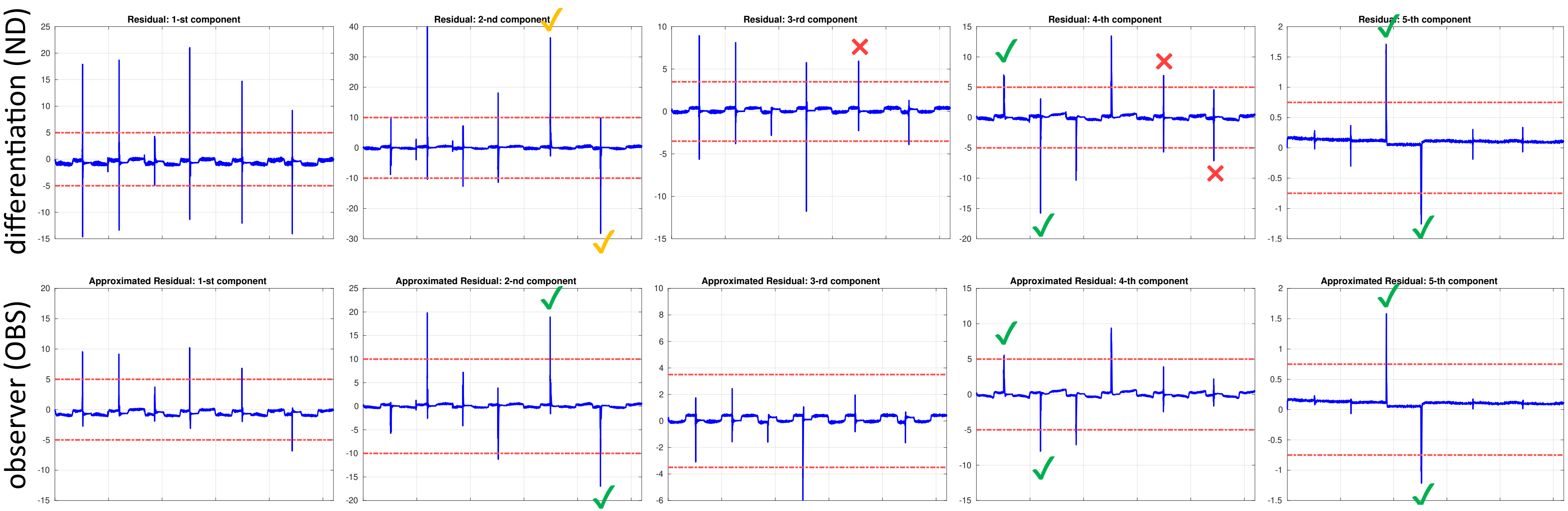

Robots with elastic joints

A more complete dynamic model

- remove the extra modeling assumption by Spong (ASME Transactions JDSMC 1987)
  - include also the inertial couplings between motors and links
  - the additional terms become relevant only for low reduction ratios n_{ri}
    - **structural property**: the complete model is feedback linearizable **only** when allowing dynamic state feedback

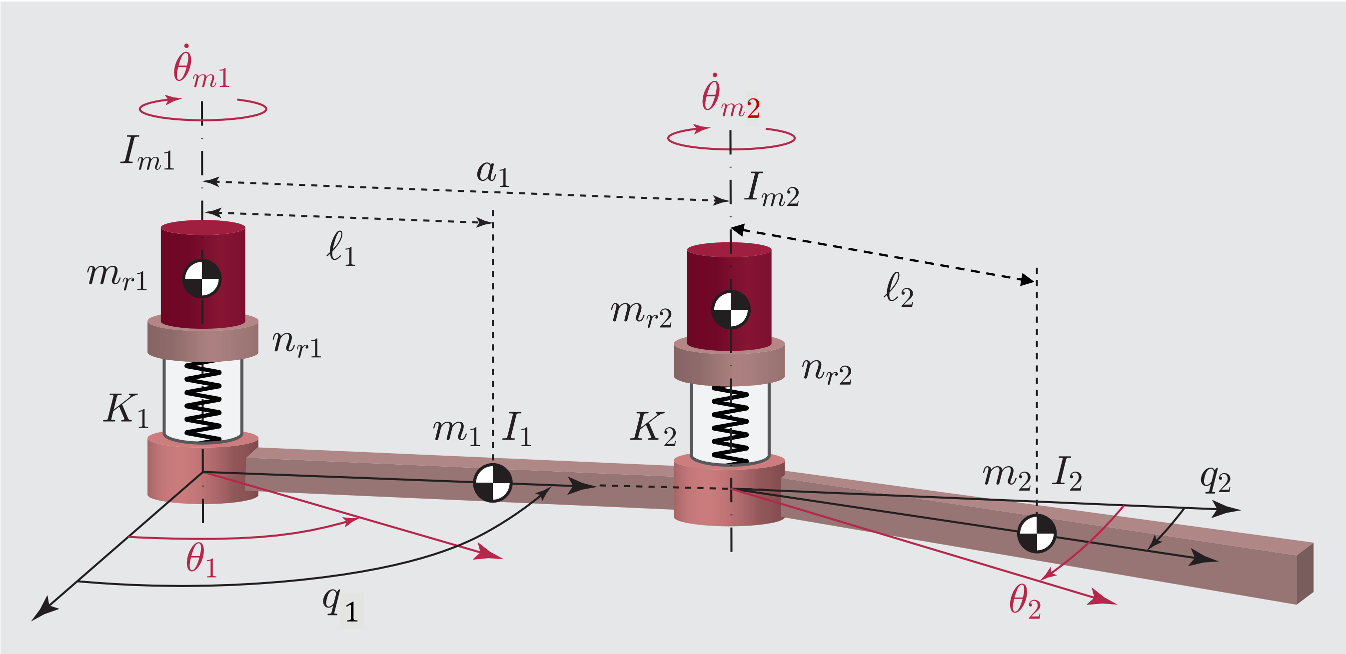

always strictly upper-triangular

$$T_{m2} = \frac{1}{2} m_{r2} a_1^2 \dot{q}_1^2 + \frac{1}{2} I_{m2} \left(\dot{q}_1 + \dot{\theta}_{m2}\right)^2 \quad \leftarrow \quad \left[\dot{\theta}_{m2} = n_{r2}\dot{\theta}_2\right]$$

$$= \frac{1}{2}\left(m_{r2} a_1^2 + I_{m2}\right)\dot{q}_1^2 + \frac{1}{2}\left(I_{m2} n_{r2}^2\right)\dot{\theta}_2^2 + I_{m2} n_{r2}\,\dot{q}_1\dot{\theta}_2$$

with terms in $\boldsymbol{M}(\boldsymbol{q})$

diagonal term in $\boldsymbol{M_m}$

extra term in off-diagonal block $\boldsymbol{N}$ or $\boldsymbol{N}(\boldsymbol{q})$ of inertia matrix!

Robots with elastic joints

Momentum-based residual for the complete model

- case of **constant** matrix $\boldsymbol{N}$ (e.g., all planar manipulators with n revolute joints)

$$\underbrace{\begin{pmatrix} \boldsymbol{M}(\boldsymbol{q}) & \boldsymbol{N} \\ \boldsymbol{N}^T & \boldsymbol{M}_m \end{pmatrix}}_{=\mathcal{M}(\boldsymbol{q})} \begin{pmatrix} \ddot{\boldsymbol{q}} \\ \ddot{\boldsymbol{\theta}} \end{pmatrix} + \begin{pmatrix} \boldsymbol{S}(\boldsymbol{q},\dot{\boldsymbol{q}})\dot{\boldsymbol{q}} \\ \boldsymbol{0} \end{pmatrix} + \begin{pmatrix} \boldsymbol{g}(\boldsymbol{q}) \\ \boldsymbol{f}_m(\boldsymbol{q},\dot{\boldsymbol{q}}) \end{pmatrix} = \begin{pmatrix} \boldsymbol{\tau}_C + \boldsymbol{\tau}_J \\ \boldsymbol{\tau} - \boldsymbol{\tau}_J \end{pmatrix}$$

$$\boldsymbol{\tau}_J = \boldsymbol{K}(\boldsymbol{\theta} - \boldsymbol{q})$$

  - addition of **constant** terms in the robot inertia matrix does **not** generate new velocity terms, based on Christoffel symbols computation

- **new** vector residual for collision detection and isolation

$$\boldsymbol{r}_{EJ}(t) = \boldsymbol{K}_r \left(\boldsymbol{M}(\boldsymbol{q})\dot{\boldsymbol{q}} + \boldsymbol{N}\dot{\boldsymbol{\theta}} - \int_0^t \left(\boldsymbol{\tau}_J + \boldsymbol{S}^T(\boldsymbol{q},\dot{\boldsymbol{q}})\dot{\boldsymbol{q}} - \boldsymbol{g}(\boldsymbol{q}) + \boldsymbol{r}_{\mathrm{EJ}}\right) ds \right)$$

$$\boldsymbol{K}_r > 0, \text{diagonal}$$

$\Rightarrow$ $$\dot{\boldsymbol{r}}_{EJ} = \boldsymbol{K}_r\left(\boldsymbol{\tau}_C - \boldsymbol{r}_{EJ}\right)$$

Robots with elastic joints

Momentum-based residual for the complete model

- **general** case of configuration-dependent matrix $\boldsymbol{N}(\boldsymbol{q})$

$$\begin{pmatrix} \boldsymbol{M}(\boldsymbol{q}) & \boldsymbol{N}(\boldsymbol{q}) \\ \boldsymbol{N}^T(\boldsymbol{q}) & \boldsymbol{M}_m \end{pmatrix} \begin{pmatrix} \ddot{\boldsymbol{q}} \\ \ddot{\boldsymbol{\theta}} \end{pmatrix} + \begin{pmatrix} \boldsymbol{c}_q(\boldsymbol{q}, \dot{\boldsymbol{q}}, \dot{\boldsymbol{\theta}}) \\ \boldsymbol{c}_\theta(\boldsymbol{q}, \dot{\boldsymbol{q}}) \end{pmatrix} + \begin{pmatrix} \boldsymbol{g}(\boldsymbol{q}) \\ \boldsymbol{f}_m(\boldsymbol{q}, \dot{\boldsymbol{q}}) \end{pmatrix} = \begin{pmatrix} \boldsymbol{\tau}_C + \boldsymbol{\tau}_J \\ \boldsymbol{\tau} - \boldsymbol{\tau}_J \end{pmatrix}$$

$= \mathcal{M}(\boldsymbol{q})$ Coriolis/centrifugal $\boldsymbol{\tau}_J = \boldsymbol{K}(\boldsymbol{\theta} - \boldsymbol{q})$

  - rotors of the motors are modeled as **balanced** uniform bodies (with center of mass on rotation axis) ⇒ the robot inertia matrix and the gravity vector are functions of **link variables $\boldsymbol{q}$** only
  - dependencies in the **quadratic velocity terms** follow from Christoffel symbols (tedious) computations

$$\boldsymbol{c}(\boldsymbol{q}, \dot{\boldsymbol{q}}) = \begin{pmatrix} \boldsymbol{c}_q(\boldsymbol{q}, \dot{\boldsymbol{q}}, \dot{\boldsymbol{\theta}}) \\ \boldsymbol{c}_\theta(\boldsymbol{q}, \dot{\boldsymbol{q}}) \end{pmatrix} = \begin{pmatrix} \boldsymbol{S}_{qq}(\boldsymbol{q}, \dot{\boldsymbol{q}}, \dot{\boldsymbol{\theta}}) & \boldsymbol{S}_{q\theta}(\boldsymbol{q}, \dot{\boldsymbol{q}}) \\ \boldsymbol{S}_{\theta q}(\boldsymbol{q}, \dot{\boldsymbol{q}}) & \boldsymbol{0} \end{pmatrix} \begin{pmatrix} \dot{\boldsymbol{q}} \\ \dot{\boldsymbol{\theta}} \end{pmatrix} = \mathcal{S}(\boldsymbol{q}, \dot{\boldsymbol{q}}, \dot{\boldsymbol{\theta}}) \begin{pmatrix} \dot{\boldsymbol{q}} \\ \dot{\boldsymbol{\theta}} \end{pmatrix}$$

$$\dot{\mathcal{M}}(\boldsymbol{q}) = \mathcal{S}(\boldsymbol{q}, \dot{\boldsymbol{q}}) + \mathcal{S}^T(\boldsymbol{q}, \dot{\boldsymbol{q}})$$ extended skew-symmetry property

- **new** vector residual for collision detection and isolation

$$\boldsymbol{r}_{EJ}(t) = \boldsymbol{K}_r \left(\boldsymbol{M}(\boldsymbol{q})\dot{\boldsymbol{q}} + \boldsymbol{N}(\boldsymbol{q})\dot{\boldsymbol{\theta}} - \int_0^t \left(\boldsymbol{\tau}_J + \boldsymbol{S}_{qq}^T(\boldsymbol{q}, \dot{\boldsymbol{q}}, \dot{\boldsymbol{\theta}})\dot{\boldsymbol{q}} + \boldsymbol{S}_{q\theta}^T(\boldsymbol{q}, \dot{\boldsymbol{q}})\dot{\boldsymbol{\theta}} - \boldsymbol{g}(\boldsymbol{q}) + \boldsymbol{r}_{EJ} \right) ds \right)$$

$\boldsymbol{K}_r > 0, \text{diagonal}$

➡ $\dot{\boldsymbol{r}}_{EJ} = \boldsymbol{K}_r \left(\boldsymbol{\tau}_C - \boldsymbol{r}_{EJ} \right)$

Robots with flexible links

Motivating example: FLEXARM

- **FLEXARM** is a two-link planar direct-drive robot with revolute joints and a **flexible forearm**
  - the first link is very stiff, as opposed to the forearm
  - distributed flexibility is relevant only in the horizontal plane of motion (bending)
  - simple structure, but already with the most relevant nonlinear and coupling dynamic effects
- robot **state** (a finite-dimensional approximation!) **can be measured** by a combination of
  - motor encoders
  - optical sensors
  - strain gauges

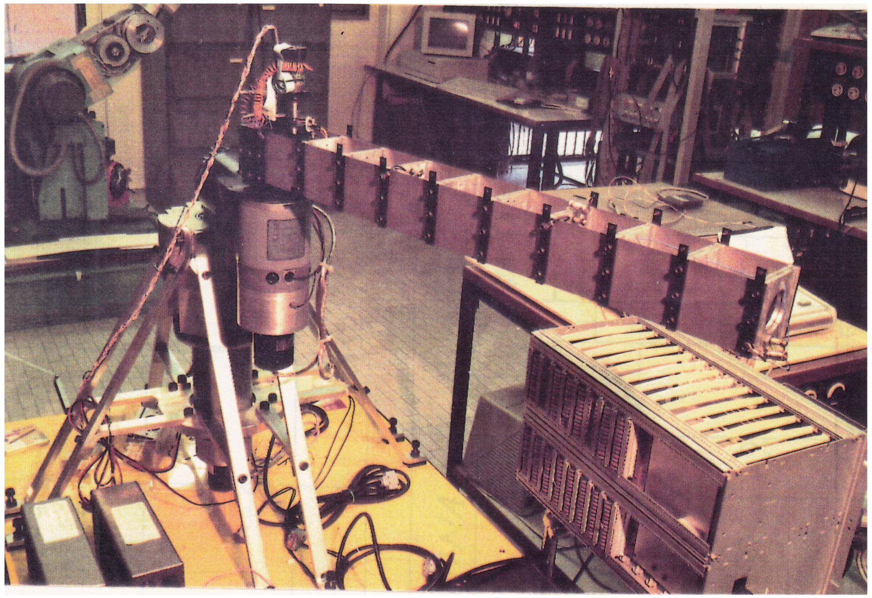

@Sapienza
Robotics Lab, 1990

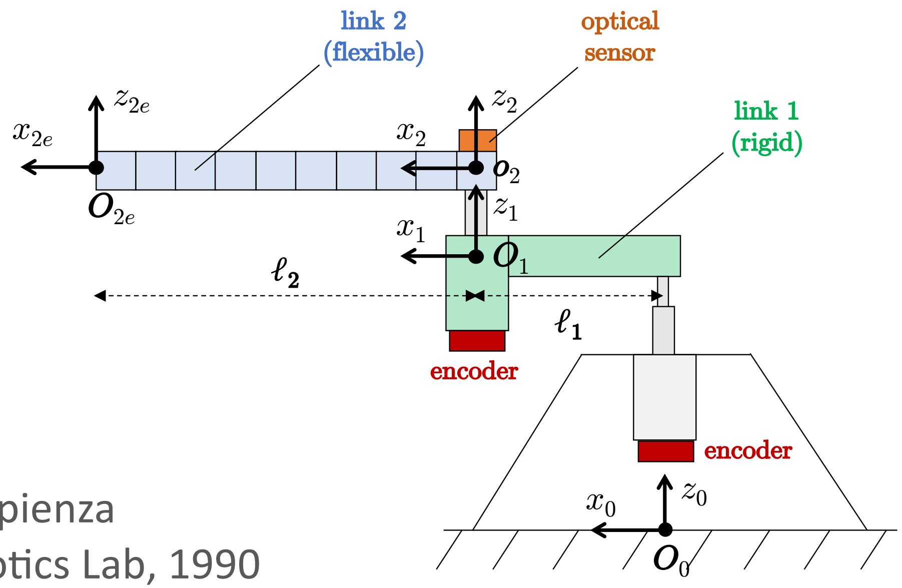

A two-link robot with a flexible forearm

Relevant system variables

- system variables
  - **first rigid link:** joint angle θ_1
  - **second flexible link:**
    - modeled as a bending Euler-Bernoulli beam with dynamic boundary conditions
    - distributed flexibility approximated with n_e modal eigenfunctions ϕ_i and variables δ_i

$$w(s,t) = \sum_{i=1}^{n_e} \phi_i(s)\delta_i(t) = \boldsymbol{\phi}^T(s)\,\boldsymbol{\delta}(t) \qquad s \in [0, \ell_2]$$

    - joint angle θ_2 pointing at the CoM of forearm

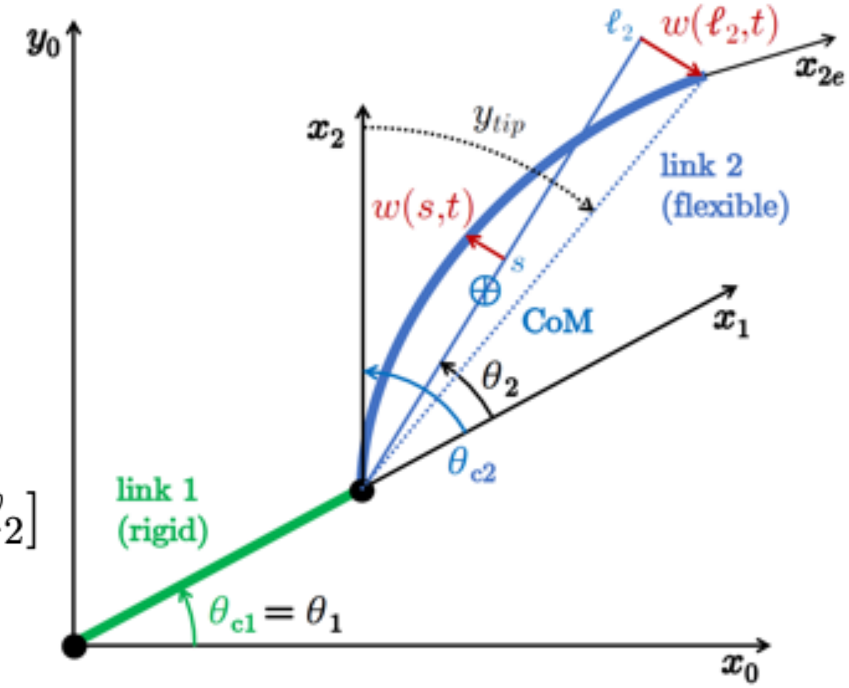

- measurable quantities

$$\boldsymbol{\theta}_c = \begin{pmatrix} \theta_{c1} \\ \theta_{c2} \end{pmatrix} = \begin{pmatrix} \theta_1 \\ \theta_2 + \sum_{i=1}^{n_e} \phi'_{i0}\delta_i \end{pmatrix} \qquad y_{tip} = \left(\theta_2 + \frac{w(\ell_2,t)}{\ell_2}\right) - \theta_{c2} = \sum_{i=1}^{n_e} \left(\frac{\phi_{ie}}{\ell_2} - \phi'_{i0}\right)\delta_i$$

joint angles **clamped** to the motors (measured by encoders)

tip deflection of the forearm (measured by an optical sensor at the link base)

A two-link robot with a flexible forearm

Dynamic model

in the following $n_e = 2$ modes

generalized coordinates

$$\boldsymbol{q} = \begin{pmatrix} \boldsymbol{\theta} \\ \boldsymbol{\delta} \end{pmatrix} = \begin{pmatrix} \theta_1 & \theta_2 & \delta_1 & \dots & \delta_{n_e} \end{pmatrix}^T \in \mathbb{R}^{2+n_e}$$

dynamic model

$$\boldsymbol{M}(\boldsymbol{q})\ddot{\boldsymbol{q}} + \boldsymbol{S}(\boldsymbol{q},\dot{\boldsymbol{q}})\dot{\boldsymbol{q}} + \boldsymbol{K}\boldsymbol{\delta} + \boldsymbol{D}\dot{\boldsymbol{\delta}} = \boldsymbol{G}\boldsymbol{\tau} + \boldsymbol{\tau}_F$$

input matrix ($\boldsymbol{G}$); motor torques ($\boldsymbol{\tau}$); actuator faults / collision torques ($\boldsymbol{\tau}_F$)

structure of terms

$$\boldsymbol{M}(\boldsymbol{q}) = \begin{pmatrix} \boldsymbol{M}_{\theta\theta}(\theta_2, \boldsymbol{\delta}) & \boldsymbol{M}_{\theta\delta}(\theta_2) \\ \boldsymbol{M}_{\theta\delta}^T(\theta_2) & \boldsymbol{I}_{n_e \times n_e} \end{pmatrix}$$

due to modal normalization

$$\boldsymbol{S}(\boldsymbol{q},\dot{\boldsymbol{q}}) = \begin{pmatrix} \boldsymbol{S}_{\theta\theta} & \boldsymbol{S}_{\theta\delta} \\ \boldsymbol{S}_{\delta\theta}^T & \boldsymbol{S}_{\delta,\delta} \end{pmatrix}$$

… with skew-symmetric property

$$\boldsymbol{K} = \begin{pmatrix} \boldsymbol{O}_{2\times 2} & \boldsymbol{O}_{2\times n_e} \\ \boldsymbol{O}_{n_e\times 2} & \boldsymbol{K}_\delta \end{pmatrix}$$

stiffness matrix

$$\boldsymbol{D} = \begin{pmatrix} \boldsymbol{O}_{2\times 2} & \boldsymbol{O}_{2\times n_e} \\ \boldsymbol{O}_{n_e\times 2} & \boldsymbol{D}_\delta \end{pmatrix}$$

modal damping (+ joint viscous friction)

$$\boldsymbol{G} = \begin{pmatrix} \boldsymbol{I}_{2\times 2} \\ \boldsymbol{G}_\delta \end{pmatrix}$$

input matrix

A. De Luca, L. Lanari, P. Lucibello, S. Panzieri, G. Ulivi "Control experiments on a two-link robot with a flexible forearm" CDC 1990

Actuator fault/collision detection and isolation

Momentum-based residuals for robots with flexible links

- generalized momentum of a manipulator with **flexible links**

$$\boldsymbol{p} = \begin{pmatrix} \boldsymbol{p}_\theta \\ \boldsymbol{p}_\delta \end{pmatrix} = \begin{pmatrix} \boldsymbol{M}_{\theta\theta}\,\dot{\boldsymbol{\theta}} + \boldsymbol{M}_{\theta\delta}\,\dot{\boldsymbol{\delta}} \\ \boldsymbol{M}_{\theta\delta}^T\,\dot{\boldsymbol{\theta}} + \boldsymbol{M}_{\delta\delta}\,\dot{\boldsymbol{\delta}} \end{pmatrix} = \boldsymbol{M}(\boldsymbol{q})\dot{\boldsymbol{q}}$$

- **vector** residual for actuator faults or collisions detection and isolation

$$\boldsymbol{r}_\theta(t) = \boldsymbol{K}_r \left(\boldsymbol{p}_\theta - \int_0^t \left(\boldsymbol{\tau} + \boldsymbol{S}_{\theta\theta}^T\,\dot{\boldsymbol{\theta}} + \boldsymbol{S}_{\theta\delta}^T\,\dot{\boldsymbol{\delta}} + \boldsymbol{r}_\theta \right) ds \right) \in \mathbb{R}^2$$

$$\Rightarrow \quad \dot{\boldsymbol{r}}_\theta = \boldsymbol{K}_r\left(\boldsymbol{\tau}_F - \boldsymbol{r}_\theta\right)$$

- … a **complete** residual $\boldsymbol{r} \in \mathbb{R}^{2+n_e}$ could be designed, but r_θ is already sufficient
- **threshold** condition for **detection** of an actuator fault/link collision event

$$\exists i \in \{1,2\} \quad \text{s.t.} \quad |r_i| \geq r_{\text{th}}$$

- usual rules for **isolation** (= **index** of the largest/only component exceeding …)

C. Gaz, A. Cristofaro, A. De Luca "Detection and isolation of actuator faults and collisions for a flexible robot arm" CDC 2020

Actuator faults

Simulation results (in all cases: under **PD control** for tracking sinusoidal **joint** trajectories)

- fault on motor 1: 90% of torque loss from t_F = 5 s

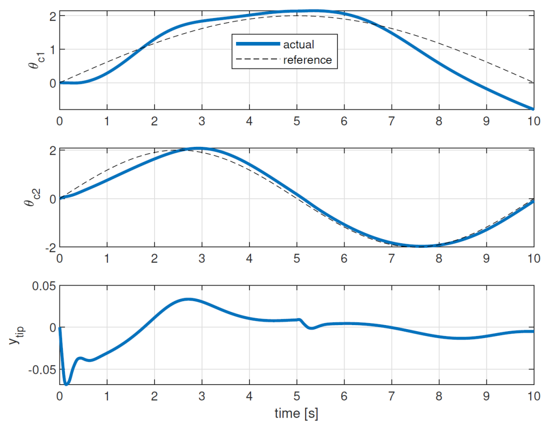

outputs

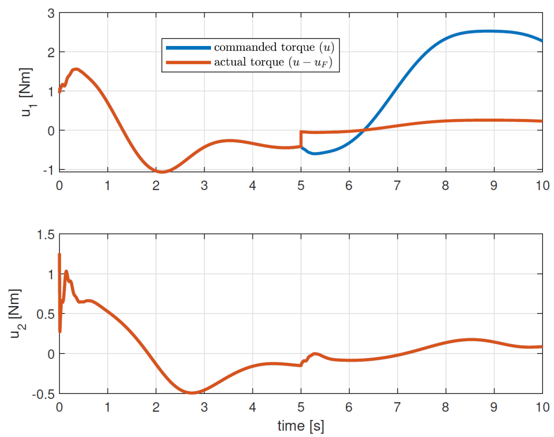

torques

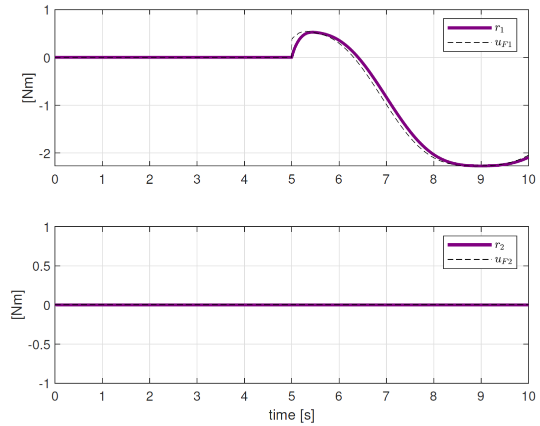

residuals

- fault on motor 2: 90% of torque loss from t_F = 5 s

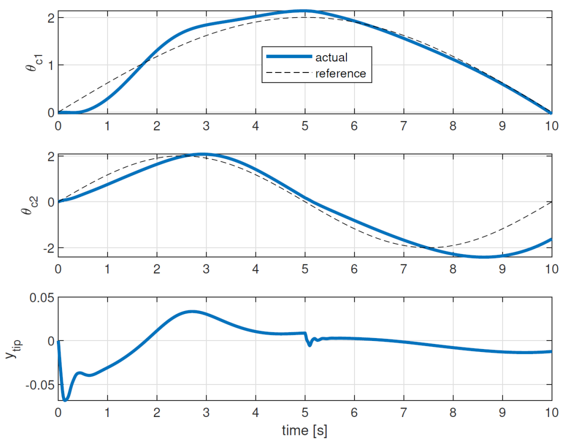

outputs

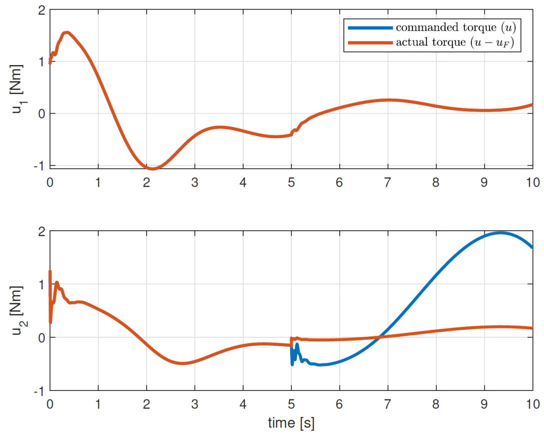

torques

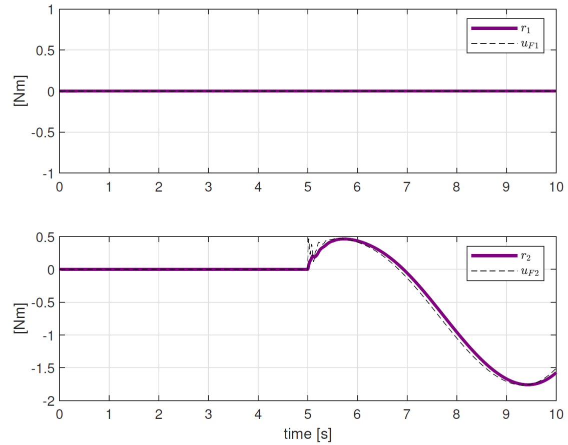

residuals

Actuator faults

Simulation results

- **concurrent** faults on both motors: 20% of torque loss for motor 1 from t_{F1} = 5 s and for motor 2 from t_{F2} = 10 s

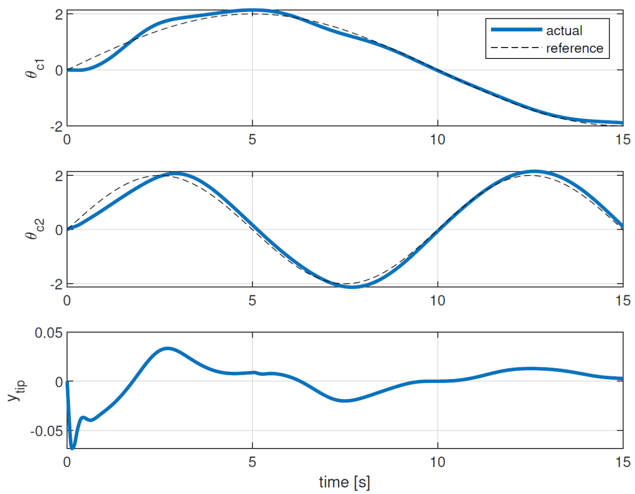

outputs

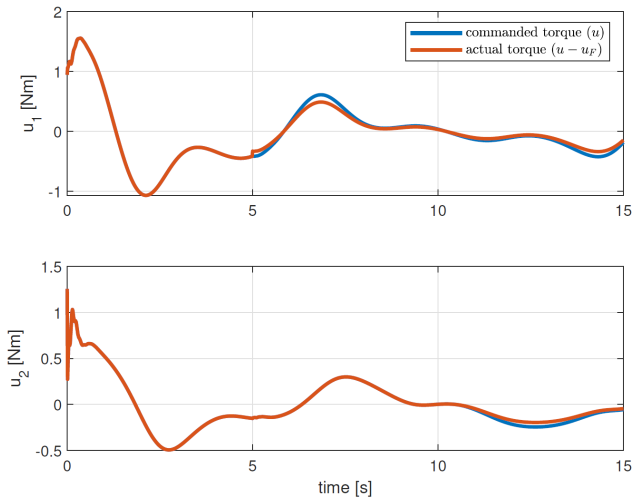

torques

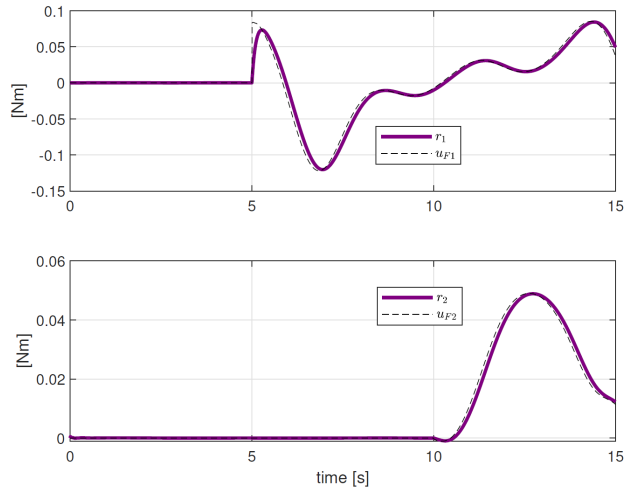

residuals

➡ it is always possible to **detect** and **isolate** the actuator faults

Link collisions

Simulation results

- collisions on both links
  - external force $\boldsymbol{F}_{\mathrm{C}} = (1 \quad 1)^T$ applied to the end of the (rigid) link 1 for $t_{\mathrm{F1}} \in [10, 12]$ s
  - external force $\boldsymbol{F}_{\mathrm{C}} = (1 \quad 1)^T$ applied to the tip of the (flexible) link 2 for $t_{\mathrm{F2}} \in [25, 27]$ s
  - relation from $\boldsymbol{F}_{\mathrm{C}}$ to $\boldsymbol{\tau}_{\mathrm{C}}$ with transpose of the **contact Jacobian:** $\boldsymbol{\tau}_C \, (= \boldsymbol{\tau}_F) = \boldsymbol{J}_C^T(\boldsymbol{q})\boldsymbol{F}_C$

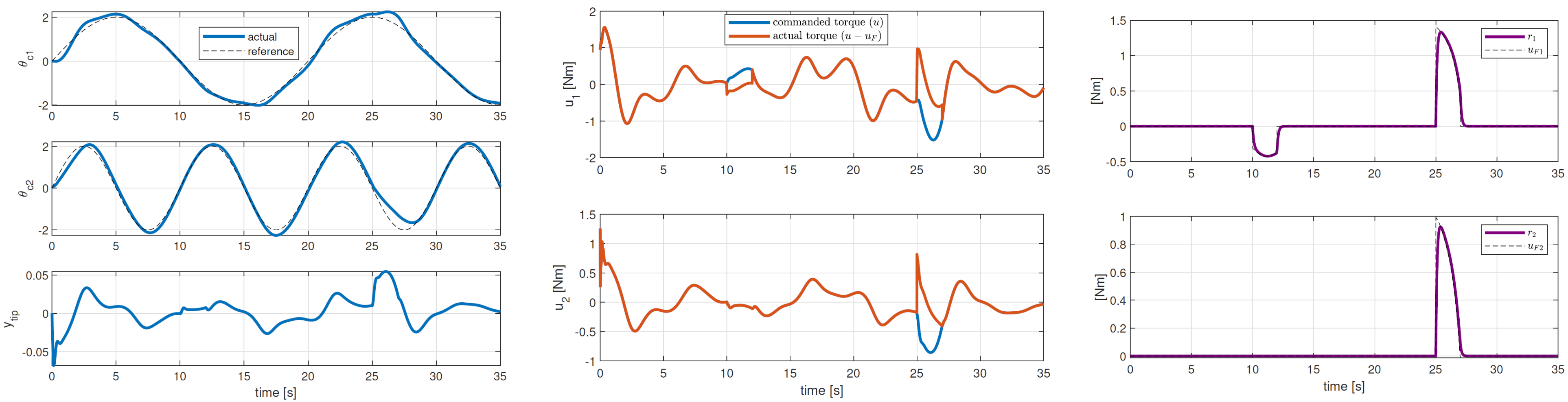

outputs torques residuals

➡ in most cases (!?), it is possible to **detect** and **isolate** the link collisions

➡ … but it is **not** possible to discriminate actuator faults from link collisions

Nonlinear state observer

General setup

- design of **state observers** for input-affine nonlinear system

$$\begin{aligned}\dot{\boldsymbol{x}} &= \boldsymbol{f}(\boldsymbol{x}) + \boldsymbol{g}(\boldsymbol{x})\boldsymbol{u} \\ \boldsymbol{y} &= \boldsymbol{h}(\boldsymbol{x})\end{aligned} \qquad \boldsymbol{u} \in \mathbb{R}^{\rho},\ \boldsymbol{x} \in \mathbb{R}^{\nu},\ \boldsymbol{y} \in \mathbb{R}^{\mu}$$

- (repeated) Lie derivatives of functions along a vector field

$$L_f h_j(\boldsymbol{x}) = \frac{\partial h_j}{\partial \boldsymbol{x}} \boldsymbol{f}(\boldsymbol{x}) \qquad L_f^k h_j(\boldsymbol{x}) = L_f \left(L_f^{k-1} h_j(\boldsymbol{x}) \right)$$

- compute the **relative degree** of each of the system (measurable) outputs

$$\begin{aligned}&\forall\, \boldsymbol{x} \in \Omega \subset \mathbb{R}^{\nu} \qquad L_g L_f^k h_j(\boldsymbol{x}) = 0 \qquad \forall k = 0, 1, \ldots, r_j - 2 \\ &\exists\, \bar{\boldsymbol{x}} \in \Omega \subset \mathbb{R}^{\nu}: \quad L_g L_f^{r_j - 1} h_j(\bar{\boldsymbol{x}}) \neq 0\end{aligned}$$

- if the system has **vector relative degree**

$$r = r_1 + \cdots + r_{\mu} = \nu$$

a Luenberger-type nonlinear state observer can be designed with local exponential convergence

see e.g. A. Isidori "Nonlinear Control Systems" 3rd Edition 1995

A drift-observability nonlinear observer

General setup

- when the system is **autonomous**, a **drift-observability map** having full rank could be found, which allows the design of a nonlinear state observer with similar convergence properties

$$\boldsymbol{\Phi}_j^T(\boldsymbol{x}) = \begin{pmatrix} h_j(\boldsymbol{x}) & L_f h_j(\boldsymbol{x}) & \dots & L_f^{\nu_j - 1} h_j(\boldsymbol{x}) \end{pmatrix}^T \in \mathbb{R}^{\nu_j}$$

$$\boldsymbol{J}_\Phi(\boldsymbol{z}) = \left.\frac{\partial \boldsymbol{\Phi}}{\partial \boldsymbol{x}}\right|_{\boldsymbol{x} = \boldsymbol{\Phi}^{-1}(\boldsymbol{z})} \quad \text{nonsingular} \qquad \nu_1 + \dots + \nu_\mu = \nu$$

M. Dalla Mora, A. Germani, C. Manes "Design of state observers from a drift-observability property" IEEE Transactions on Automatic Control 2000

- if a vector relative degree **does not hold**, since the control input $\boldsymbol{u}$ is typically designed as $\boldsymbol{u}(\boldsymbol{x})$, one can look for and exploit a **drift-like observability** property

$$\dot{\boldsymbol{x}} = \boldsymbol{f}(\boldsymbol{x}) + \boldsymbol{g}(\boldsymbol{x})\boldsymbol{u}(\boldsymbol{x}) = \tilde{\boldsymbol{f}}(\boldsymbol{x}) \quad \Rightarrow \quad \dot{\boldsymbol{x}} = \boldsymbol{f}(\boldsymbol{x}) + \boldsymbol{g}(\boldsymbol{x})\boldsymbol{u}(\hat{\boldsymbol{x}})$$

$$\boldsymbol{\Phi}_j^T(\boldsymbol{x}) = \begin{pmatrix} h_j(\boldsymbol{x}) & L_{\tilde{f}} h_j(\boldsymbol{x}) & \dots & L_{\tilde{f}}^{\nu_j - 1} h_j(\boldsymbol{x}) \end{pmatrix}^T \in \mathbb{R}^{\nu_j}$$

$$\boldsymbol{J}_\Phi(\boldsymbol{z}) = \left.\frac{\partial \boldsymbol{\Phi}}{\partial \boldsymbol{x}}\right|_{\boldsymbol{x} = \boldsymbol{\Phi}^{-1}(\boldsymbol{z})} \quad \text{nonsingular} \qquad \nu_1 + \dots + \nu_\mu = \nu$$

C. Gaz, A. Cristofaro, P. Palumbo, A. De Luca "A nonlinear observer for a flexible robot arm and its use in fault and collision detection" CDC 2022

Application of the drift-like observer to the FLEXARM

Synthesis procedure (for $n_e = 2$ modes)

inputs $\quad \boldsymbol{u} = \boldsymbol{\tau} \in \mathbb{R}^2 \qquad \rho = 2$

measured outputs

$$\boldsymbol{y} = \boldsymbol{h}(\boldsymbol{x}) \quad \Rightarrow \quad \boldsymbol{y} = \begin{pmatrix} \theta_1 \\ \theta_{c2} \\ y_{tip} \end{pmatrix} = \boldsymbol{h}(\boldsymbol{q}) \qquad \mu = 3$$

in mechanical systems with outputs $h_j(q)$

$$L_{\tilde{f}} h_j(\boldsymbol{x}) = L_f h_j(\boldsymbol{x})$$

no vector relative degree

$$r = r_1 + r_2 + r_3 = 2 + 2 + 2 = 6 < 8 = \nu$$

PD control with observed state(s)

$$\boldsymbol{u} = \boldsymbol{u}(\hat{\boldsymbol{x}}) \quad \Rightarrow \quad \boldsymbol{\tau} = \boldsymbol{K}_P\left(\boldsymbol{\theta}_{c,des} - \boldsymbol{\theta}_c\right) + \boldsymbol{K}_D\left(\dot{\boldsymbol{\theta}}_{c,des} - \dot{\hat{\boldsymbol{\theta}}}_c\right)$$

drift-like observability map

$$\boldsymbol{z} = \boldsymbol{\Phi}(\boldsymbol{x}) \quad \Rightarrow \quad \boldsymbol{\Phi}(\boldsymbol{q}, \dot{\boldsymbol{q}}) = \begin{pmatrix} \theta_1(\boldsymbol{q}) & L_f\theta_1(\dot{\boldsymbol{q}}) & L_{\tilde{f}}^2\theta_1(\boldsymbol{q}, \dot{\boldsymbol{q}}) \\ \theta_{c2}(\boldsymbol{q}) & L_f\theta_{c2}(\dot{\boldsymbol{q}}) & L_{\tilde{f}}^2\theta_{c2}(\boldsymbol{q}, \dot{\boldsymbol{q}}) \\ y_{tip}(\boldsymbol{q}) & L_f y_{tip}(\dot{\boldsymbol{q}}) & \end{pmatrix}^T$$

$$\nu_1 + \nu_2 + \nu_3 = 3 + 3 + 2 = 8 = \nu \qquad \boldsymbol{J}_\Phi(\boldsymbol{z}) = \left.\frac{\partial \boldsymbol{\Phi}}{\partial \boldsymbol{x}}\right|_{\boldsymbol{x} = \boldsymbol{\Phi}^{-1}(\boldsymbol{z})} \quad \text{nonsingular}$$

→ nonlinear observer

$$\dot{\hat{\boldsymbol{x}}} = \boldsymbol{f}(\hat{\boldsymbol{x}}) + \boldsymbol{g}(\hat{\boldsymbol{x}})\boldsymbol{u}(\hat{\boldsymbol{x}}) + \boldsymbol{J}_\Phi^{-1}(\hat{\boldsymbol{x}})\boldsymbol{\Gamma}\left(\boldsymbol{y} - \boldsymbol{h}(\hat{\boldsymbol{x}})\right)$$

C. Gaz, A. Cristofaro, P. Palumbo, A. De Luca “A nonlinear observer for a flexible robot arm and its use in fault and collision detection” CDC 2022

Dynamic feedback control

Simulation results: observer performance

- a PD law with **observed** velocity is applied to track the desired joint trajectories

$$\theta_{c1,des}(t) = 2\sin 0.05\pi t$$
$$\theta_{c2,des}(t) = 2\sin 0.1\pi t$$

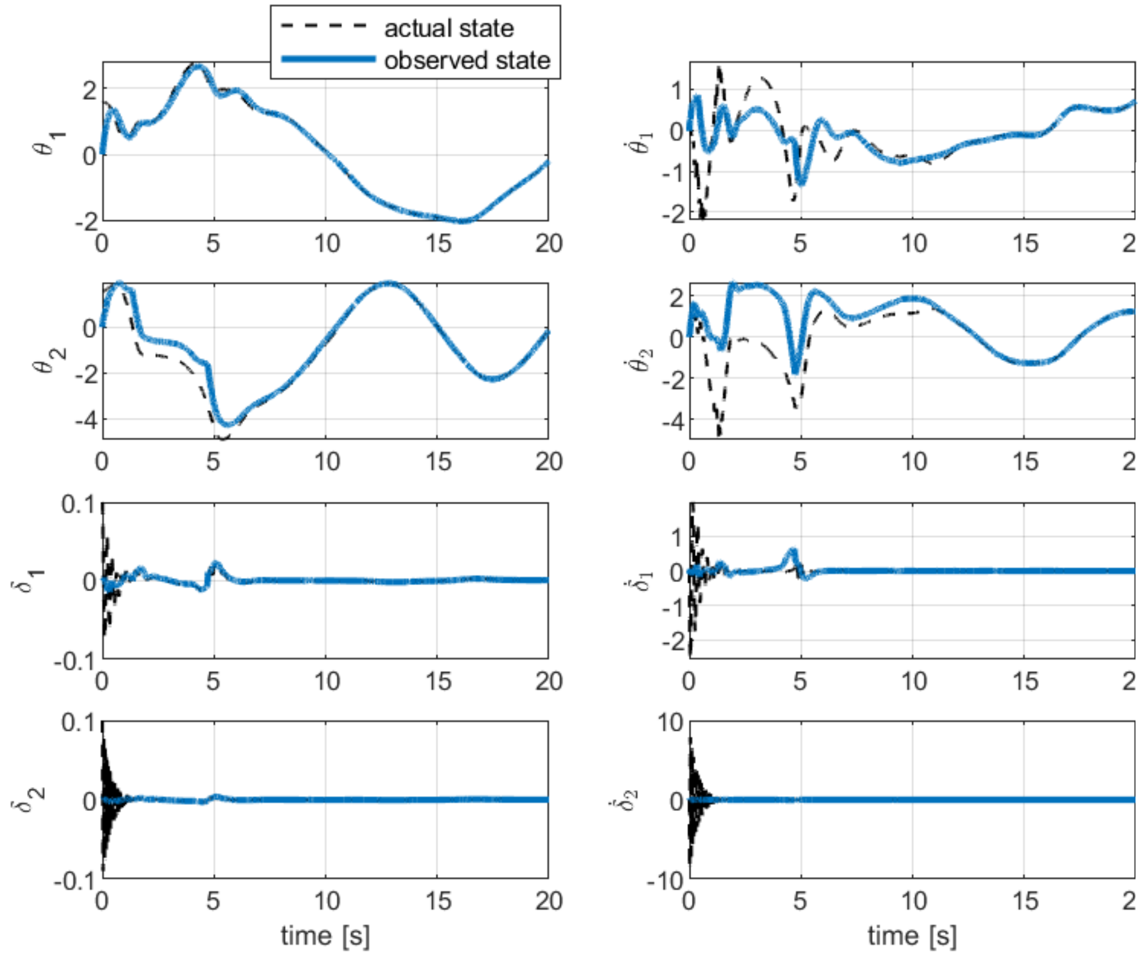

estimation error convergence for the 8 states

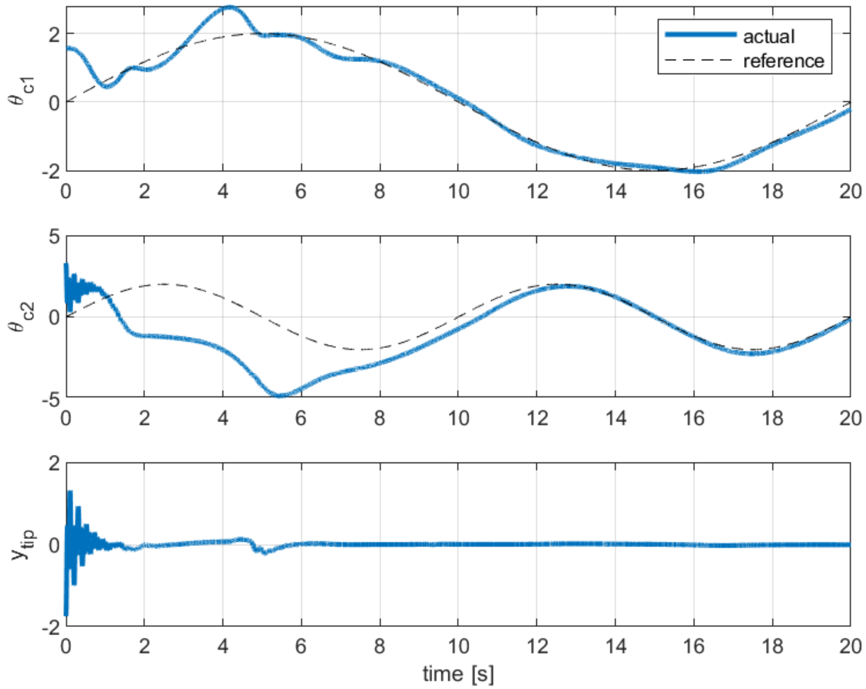

tracking error convergence
for the 3 outputs

Actuator fault detection

Simulation results: measurable observer error as monitoring signal

- an abrupt fault occurs for motor 1 at time t = 12 [s], with a 90% power loss

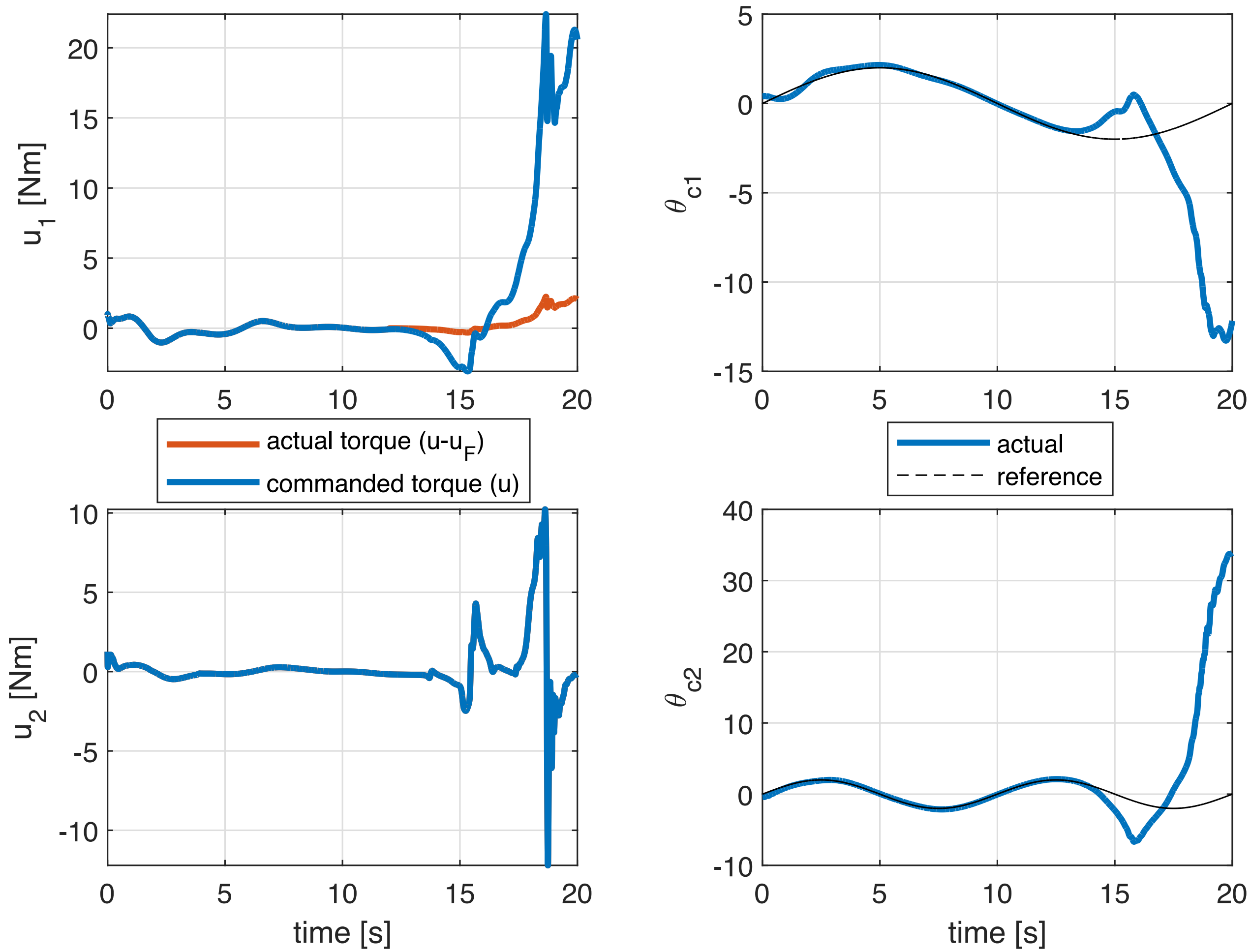

commanded/actual torques and controlled outputs

monitoring signal

$$\epsilon = \left(\theta_c - \hat{\theta}_c\right)^T \left(\theta_c - \hat{\theta}_c\right)$$

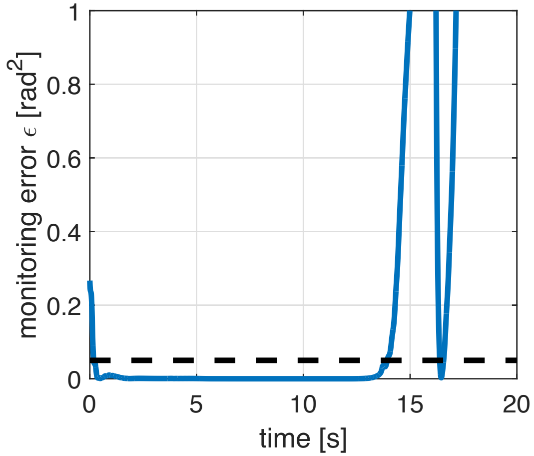

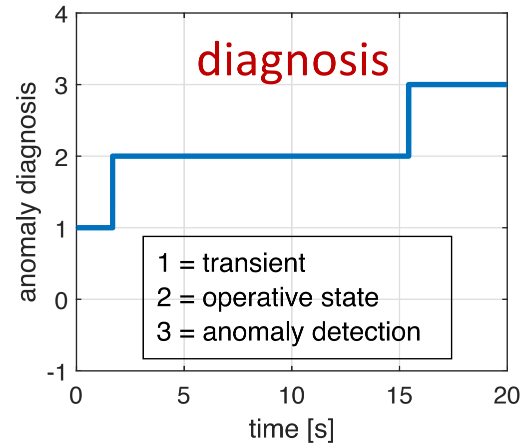

Link collision detection

Simulation results: measurable observer error as monitoring signal

- contact force applied on link 1 from t = 10 to 12 s and on link 2 from t = 25 to 27 s

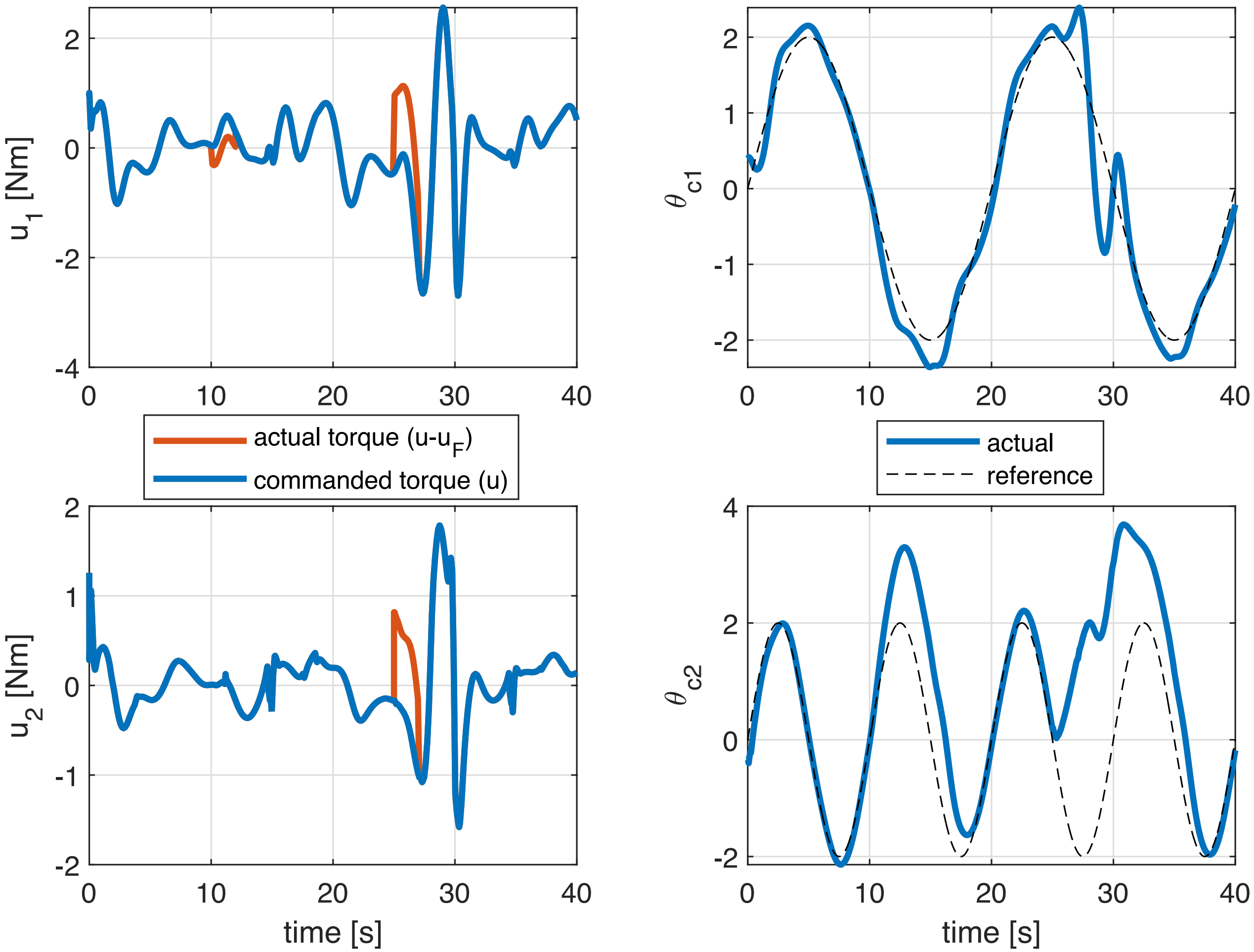

commanded/actual torques and controlled outputs

monitoring signal

$$\epsilon = \left(\theta_c - \hat{\theta}_c\right)^T \left(\theta_c - \hat{\theta}_c\right)$$

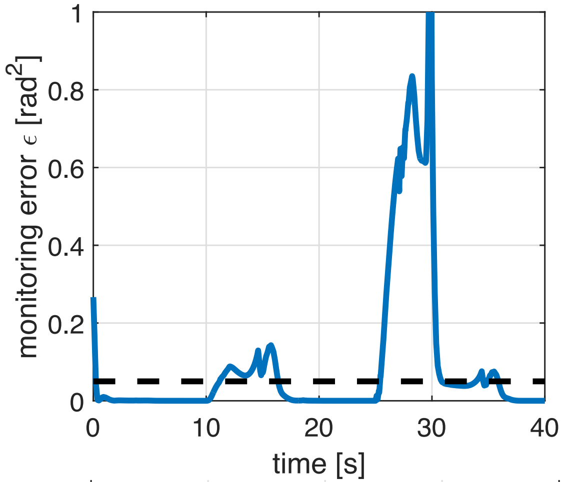

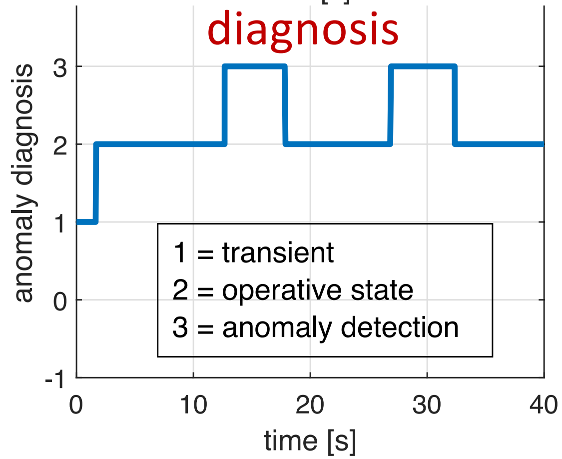

Conclusions

Take-home messages

- a physically-based residual approach (momentum/energy) to detect and isolate missing dynamic terms in robots (faults, collisions, unmodeled motor friction, …)
  - widely used in research and industry (DLR LWR/humanoids, KUKA iiwa, PAL Robotics, …), often "rediscovered" in later papers under various forms (e.g., disturbance observer)
  - applies equally well to different robotic systems – arms, UAVs (in contact!), humanoids – including manipulators with flexible elements (joints, links) and deformable soft robots!!
  - exact (decoupled) FDI in mechanical systems: max # faults = # generalized coordinates
- main application in safe physical Human-Robot Interaction (pHRI)
  - localization of contact point(s) and identification of Cartesian collision/contact forces
    - sometimes for free ⟶ combined with particle filters ⟶ using RGB-D or vision sensors
  - classification problems
    - distinguishing intentional contacts (for collaboration) from accidental collisions (fast reaction)
    - severity of actuator faults (for on-line system reconfiguration)
- being model-based, the main limitation is robustness to uncertainty
  - requires good dynamic models – especially difficult is capturing friction in rigid robots
  - combine multiple FDI approaches: model-based, signal-based, and isolation logics
  - go adaptive? use machine learning techniques?

Additional bibliography

Download pdf for personal use at www.diag.uniroma1.it/deluca/Publications

- more papers [2004-17]

A. De Luca, R. Mattone "An adapt-and-detect actuator FDI scheme for robot manipulators" ICRA 2004

A. De Luca, R. Mattone "An identification scheme for robot actuator faults " IROS 2005

L. Le Tien, A. Albu-Schäffer, A. De Luca, G. Hirzinger "Friction observer and compensation for control of robots with joint torque measurements" IROS 2008

A. De Luca, L. Ferrajoli "A modified Newton-Euler method for dynamic computations in robot fault detection and control" ICRA 2009

A. De Luca, F. Flacco "Integrated control for pHRI: Collision avoidance, detection, reaction and collaboration" BioRob 2012 (Best Paper Award)

M. Geravand, F. Flacco, A. De Luca,"Human-robot physical interaction and collaboration using an industrial robot with a closed control architecture," ICRA 2013

E. Magrini, F. Flacco, A. De Luca "Estimation of contact forces using a virtual force sensor" IROS 2014

E. Magrini, F. Flacco, A. De Luca "Control of generalized contact motion and force in physical human-robot interaction" ICRA 2015

E. Magrini, A. De Luca "Hybrid force/velocity control for physical human-robot collaboration tasks" IROS 2016

G. Buondonno, A. De Luca "Combining real and virtual sensors for measuring interaction forces and moments acting on a robot" IROS 2016

E. Magrini, A. De Luca "Human-robot coexistence and contact handling with redundant robots" IROS 2017

… bibliography and video

Download pdf for personal use at www.diag.uniroma1.it/deluca/Publications

- more papers [2018-21]

C. Gaz, E. Magrini, A. De Luca "A model-based residual approach for human-robot collaboration during manual polishing operations" Mechatronics 2018

E. Magrini, F. Ferraguti, A.J. Ronga, F. Pini, A. De Luca, F. Leali "Human-robot coexistence and interaction in open industrial cells" Robotics and Computer-Integrated Manufacturing 2020

M. Iskandar, O. Eiberger, A. Albu-Schäffer, A. De Luca, A. Dietrich "Collision detection and localization for the DLR SARA robot with sensing redundancy" ICRA 2021

M. Pennese, C. Gaz, M. Capotondi, V. Modugno, A. De Luca "Identification of robot dynamics from motor currents/torques with unknown signs," I-RIM 2021 (Best Student Paper Award)

- videos

F. Flacco, A. De Luca "Safe physical human-robot collaboration" IROS 2013 (Best Video Award Finalist)

YouTube channel: RoboticsLabSapienza **Playlist**: Physical human-robot interaction

Estimation of contact force

Sometimes, even **without** external sensing

- if contact is sufficiently “down” along the kinematic chain (**≥ 6 residuals** available), estimation of **pure contact forces** needs no external information ...

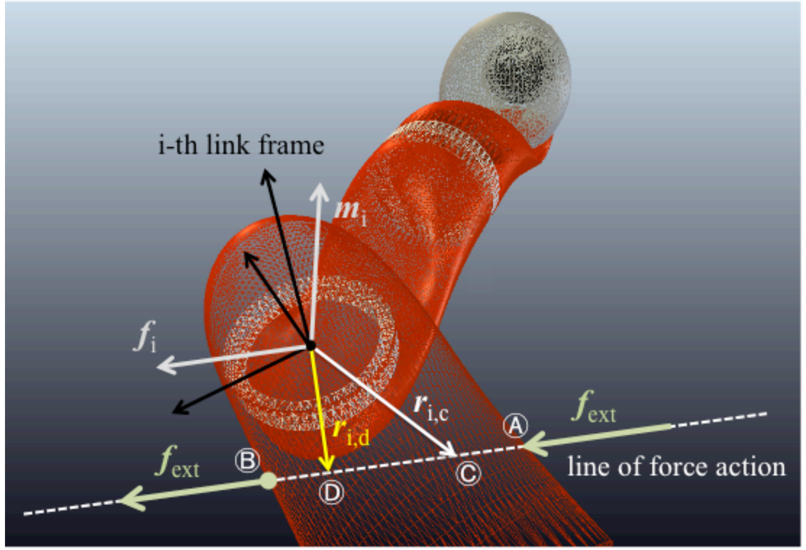

- a simple 3R planar case, with contact on different links; one can estimate:

only normal force to link,
if contact point is known
(**1** informative residual signal)

rank { J_{c1} } = 1

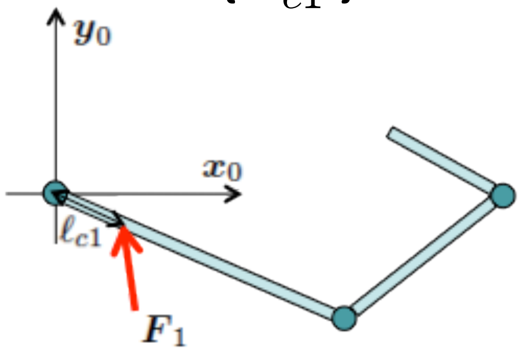

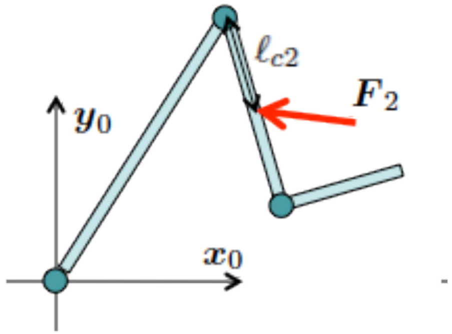

rank { J_{c2} } = 2

full force on link,
if contact point is known
(**2** informative residuals)

full force on link, **even without** knowing contact
(**3** informative residuals)

rank { J_{c3} } = 2

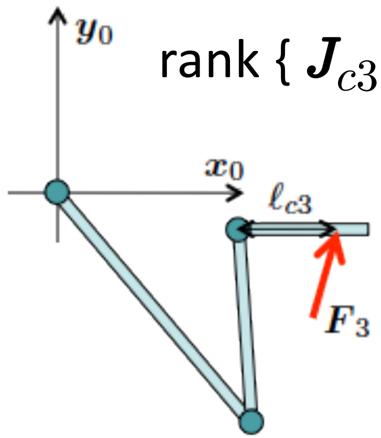

Collision or collaboration?

Distinguishing hard/accidental collisions and soft/intentional contacts

- using suitable low and high bandwidths for the residuals (first-order stable filters)

$$\dot{\boldsymbol{r}} = -\boldsymbol{K}_I \boldsymbol{r} + \boldsymbol{K}_I \boldsymbol{\tau}_K$$

- a threshold is added to prevent false collision detection during robot motion

for generic *j-th* joint

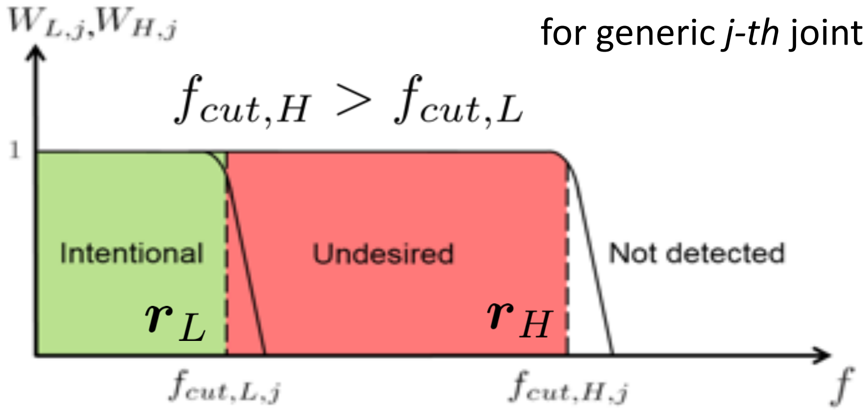

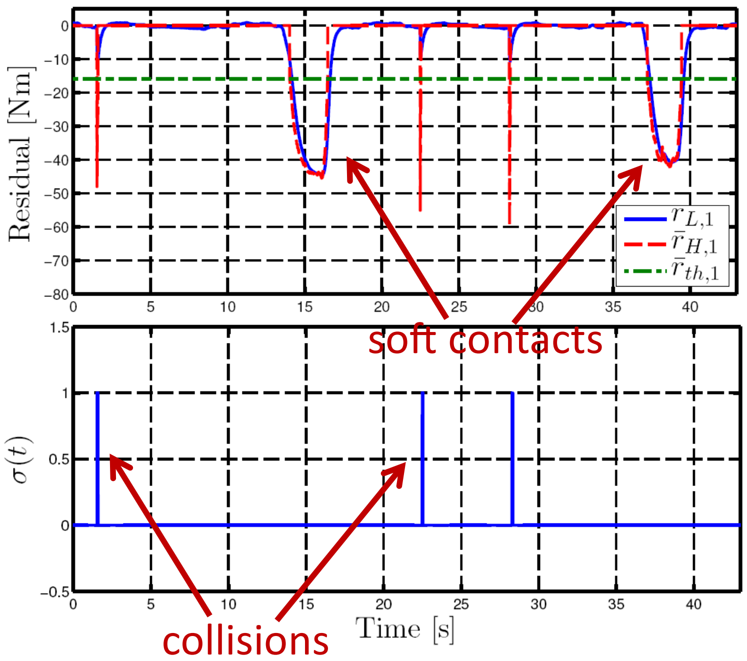

video